sustainability

MDPI

Article

Biosorption of Hexavalent Chromium by Freshwater Microalgae *Craticula subminuscula* from Aqueous Solutions

Karim Sbihi [1,2], Sara Elhamji [2,3], Siham Lghoul [4], Khalid Aziz [5], Abdelali El Maallem [1], Jamal Mabrouki [6], Mostafa El-Sheekh [7] and Faissal Aziz [2,3,*]

1 Laboratory Analysis, Modelling, Engineering, Natural Substances and Environment, Natural Substances, Health and Environment Team, Polydisciplinaire Faculty of Taroudant, Ibn Zohr University, Agadir 80000, Morocco; sbihikarim7@gmail.com (K.S.); abdelali.elmaallem@edu.uiz.ac.ma (A.E.M.)
2 National Centre for Research and Study on Water and Energy (CNEREE), Cadi Ayyad University, Marrakech 40000, Morocco; elhamjisara@gmail.com
3 Laboratory of Water, Biodiversity & Climate Changes, Semlalia Faculty of Sciences, B.P. 2390, Marrakech 40000, Morocco
4 Department of Biology, Faculty of Sciences Semlalia, Cadi Ayyad University, Marrakesh 40000, Morocco; siham.lghoul@gmail.com
5 Materials Science and Nano-Engineering (MSN) Department, VI Mohammed Polytechnic University (UM6P), Lot 660—Hay Moulay Rachid, Benguerir 43150, Morocco; khalid.aziz@um6p.ma
6 Laboratory of Spectroscopy, Molecular Modelling, Materials, Nanomaterial, Water and Environment, CERNE2D, Faculty of Science, Mohammed V University, Av. Ibn Battouta, B.P. 1014, Agdal, Rabat 10140, Morocco; jamal.mabrouki@um5r.ac.ma
7 Botany Department, Faculty of Science, Tanta University, Tanta 31527, Egypt; mostafaelsheikh@science.tanta.edu.eg
* Correspondence: f.aziz@uca.ma

Abstract: Recently, microalgae have tended to be used as a biological treatment for wastewater decontamination. The present study aimed to investigate the Cr(VI) removal using the freshwater microalgae '*Craticula subminuscula*' and their biobased adsorbant, isolated from a Moroccan river in the High Atlas Mountain. The optimum operational conditions for maximum Cr(VI) biosorption by the biobased adsorbent form (95.32%) were determined at (pH = 1.09, adsorbent dose = 10.91 mg L^{-1}, and treatment duration = 129.47 min) using response surface methodology (RSM). Under those optimal conditions, the biosorption process of Cr(VI) by *C. subminuscula* is endothermic, spontaneous and follows Langmuir and a pseudo-second-order model with a constant rate; the theoretical and experimental biosorption capacity of 0.0004 g/mg/min was 289.01 mg g^{-1} and 277.57 mg g^{-1}, respectively. Fourier Transform Infrared Spectroscopy (FTIR) analyses of the biomass and scanning electron microscopy (SEM) revealed that the principal mechanism to remove Cr(VI) by *C. subminuscula* was the affinity of Cr(VI) by the cell walls of microalgae. Thus, the positive results of desorption cycles promise increased potential utilization of these algae in continuous systems within industrial processes. The findings contribute valuable insights into the effectiveness of *C. subminuscula* as a biobased remediation agent for Cr(VI) in wastewater treatment.

Keywords: *Craticula subminuscula*; Cr(VI); biosorption; optimization; removal kinetics

Citation: Sbihi, K.; Elhamji, S.; Lghoul, S.; Aziz, K.; El Maallem, A.; Mabrouki, J.; El-Sheekh, M.; Aziz, F. Biosorption of Hexavalent Chromium by Freshwater Microalgae *Craticula subminuscula* from Aqueous Solutions. *Sustainability* **2024**, *16*, 918. https://doi.org/10.3390/su16020918

Academic Editor: Dino Musmarra

Received: 23 November 2023
Revised: 29 December 2023
Accepted: 15 January 2024
Published: 22 January 2024

1. Introduction

Heavy metal pollution of water is a serious environmental problem. One of the most common contaminants draining into natural water is chromium (Cr). According to several studies, chromium can originate from municipal and industrial wastewater generated by various activities such as leather tanning, metal finishing, electroplating, wood preserving, ore refining process, and pigmentation [1–3]. The most common forms of chromium in aquatic systems are trivalent chromium or the more dangerous hexavalent chromium. The severe toxicity of Cr(VI) and its detrimental impact on human health

and the environment are well known [4,5] and have been listed as one of the most toxic pollutants [6]. The maximum allowable concentration of total chromium in wastewater has been established due to its harmful and movable characteristics. This limit is defined by the National Environmental Quality Standards (NEQS) at 1 mg per liter, while the World Health Organization (WHO) sets a stricter guideline of 0.05 mg per liter. Additionally, the United States Environmental Protection Agency (USEPA) has determined that a concentration of up to 2.0 mg per liter is considered safe for chromium. Therefore, Cr must be effectively removed from wastewater before discharge to preserve public health. Therefore, for its elimination, an alternative treatment method is essential.

Currently, the common methods used for wastewater heavy metal remediation are chemical precipitation [7], ion exchange [8], electrodeposition, and reverse osmosis [9]. However, these methods are inconvenient because they are costly and limited, particularly in heavy metal concentrations ranging from 10 to 100 ppm [10]. Therefore, it is crucial to develop innovative, environmentally friendly processes to efficiently treat industrial wastewater containing Cr(VI) [11]. In this context, using microalgae cells for the treatment of heavy metal effluents has several benefits, such as their potential to face a variety of environmental factors related to pH, temperature, and the presence of specific ions, as the microalgae resistance to different micropollutants in wastewater [12]. To date, several microalgal and cyanobacteria species have been shown to have the potential to effectively treat wastewater that contains Cr(VI), including *Chlorella vulgaris* [13], *Scenedesmus* sp. [10,14–18], *Nannochloropsis salina* [19], and *Spirulina platensis* [20].

Microalgae have emerged as promising agents for mitigating Cr(VI) contamination, employing mechanisms such as adsorption and absorption. Adsorption involves the adherence of Cr(VI) ions to the surface of microalgal cells, while absorption entails the uptake of these ions into the cellular structure. Understanding the significance of these processes is crucial for developing effective strategies to harness the unique capabilities of microalgae in remediation efforts.

Most studies have optimized the biosorption settings by optimizing one element regardless of the other affecting parameters [21]. Therefore, insufficient experimental and modeling data regarding the effects of the parameter interactions on the effectiveness of metal biosorption is the main drawback. However, an alternative method is to use tools that include response surface methodology (RSM) for the microalgae-mediated maximal metal biosorption parameters process optimization, which is intended to provide the feasibility and applicability of the protocol. A suitable resource for conducting experiments with an extensive industrial utilization of the optimization process, RSM includes the usual mathematical and statistical tools found in fitting model simulations for the collected data according to the experimental design [22]. RSM aids in creating numerical models, evaluating the impact of the chosen variables, and identifying the combinations of the ideal variables [23]. One example is the recent estimation of the performance conditions for green microalgae (*Chlorella kessleri*), which found the biosorption of Cr, Cd, Cu, Co, and Pb from synthetic wastewater employing a hybrid response surface methodology–crow search algorithm [24].

The primary goal of the current study is to address a pivotal question: which of these mechanisms—adsorption or absorption—is more efficient for this diatom in achieving maximum Cr(VI) removal? This inquiry forms the basis for our investigation into optimizing the remediation potential of microalgae in the context of Cr(VI) removal. We assess the effects of critical parameters, individually and collectively, on the Cr(VI) biosorption process employing the diatom algae *Craticula subminuscula* as a biosorbent. The study explores the impact of biosorbent dosage, Cr(VI) concentrations, treatment duration, and pH on the Cr(VI) elimination capacity using a single-factor test. This will be performed by optimizing the critical parameters. All efforts will have been made to use the response surface methodology in order to optimize these parameters. The study will show how the critical parameters interact with one another and how they affect the bioremoval of Cr(VI). According to the experimental design in the Design Expert 13.0 software, experiment

biosorption of Cr(VI) was performed. Optimal conditions revealed that the FTIR and SEM-EDX characterization of the biomass, as well as kinetic, isothermal, and thermodynamic investigations, demonstrated the removal processes of hexavalent chromium (Cr(VI)).

2. Materials and Methods

2.1. Microalgae Absorption: Cultivation and Toxicity Test

The freshwater diatom *Craticula subminuscula* has been isolated from the Ourika River (31°16′41.0″ N, 7°41′39.1″ W) in Marrakesh, Morocco. The microalgae were cultivated in a sterile WC medium (Wright's Cryptophyta) with a pH of 7 [25]. Erlenmeyer flasks with a capacity of 2 L were used to maintain algal cultures to have enough biomass for the studies. Over a period of 10 days, the cultures were placed in a growth chamber, receiving a light intensity of 67.5 mol/m^2/s. They were maintained on a temperature-controlled shaker set at 120 rpm, following a light/dark cycle of 12 h each. During these 10 days, the cultures were aerated with an air current of 0.5 L/min at a consistent temperature of 25 °C. Cultures were routinely microscopically examined to ensure there was no contamination. These cultures were classified as axenic. Centrifugation at 10,000× *g* for five minutes separated the cells from the culture media. Finally, the cells were rinsed thrice using distilled water to leave the culture medium.

The tolerance of microalgae to heavy metals was evaluated by monitoring their growth across a range of Cr(VI) concentrations, spanning from 0 to 30 mg L^{-1}. To prepare a 100 mg per liter Cr(VI) stock solution, 0.28 g of potassium dichromate ($K_2Cr_2O_7$) was dissolved in one liter of bidistilled water. This stock solution was then diluted as required for the experiments, ensuring the pH level was controlled at a neutral value of 7, which matched typical environmental conditions. Elevated concentrations were intended to mimic the higher levels of tannery wastewater [26,27]. The same incubation conditions mentioned above were used for flasks. Cell densities and growth rates were measured to assess growth performance. Cell densities were used to calculate growth rates. Daily measurements of algal cell density were made with a hemocytometer Malassez cell. The toxic effect of Cr(VI) on microalgae was monitored using cell growth. The results of each experiment were performed in triplicate, and the median values with standard deviation are presented.

To ascertain the quantity of Cr(VI) biosorbed or removed by the living algae following the toxicity assessments, the levels of Cr(VI) in the supernatant were measured employing a colorimetric technique outlined in the standard methods. In summary, a five-milliliter sample of the microalgal culture underwent centrifugation at 5000 rpm for 5 min in order to isolate the supernatant. For the colorimetric assay, 0.2 mL of a reagent consisting of 250 mg of 1,5-diphenylcarbazide mixed in 50 mL of acetone, and 0.5 mL of 0.5 M H_3PO_4 were added to the supernatant; the reaction was allowed to proceed for 5 to 10 min for the color to develop fully. The absorbance of the resultant pink complex, which forms upon the interaction of Cr(VI) with 1,5-diphenylcarbazide, was read at a wavelength of 540 nm using a UV spectrophotometer (Evolution-201, Thermo Scientific, Waltham, MA, USA) [28]. The Cr(VI) removal percentage was then calculated using a predetermined Equation (1).

$$\text{Cr(VI) removal efficiency (\%)} = \left(\frac{C_i - C_f}{C_i}\right) \times 100 \quad (1)$$

where C_i = initial concentration of Cr(VI); and C_f = final concentration of Cr(VI).

2.2. Adsorption Experiments

2.2.1. Single-Factor Experiments

Biosorbent of biosorbants: After the exponential phase, the algal cells were centrifuged and rinsed with physiological saline. The cells were then dehydrated in an oven at 60 °C until reaching a stable weight. The derived dry biomass was preserved in a desiccator for later use as biosorbents in the adsorption experiments.

Batch biosorption equilibrium experiments investigated Cr(VI) adsorption on the algal biomass. The adsorption experiments were conducted using 250 mL flasks containing

100 mL of synthetic wastewater. Different conditions were designated for future research to maximize Cr(VI) adsorption capacity. The concentrations of Cr(VI) in tannery effluent vary between 0.1 and 38 mg L^{-1}, as claimed by Sbihi et al. [26]. Cultures conditions like pH (0.5, 1.00, 2.00, 3.00, 4.00 and 5.00), Cr(VI) concentration (0 mg L^{-1}, 10 mg L^{-1}, 15 mg L^{-1}, 20 mg L^{-1}, 25 mg L^{-1}, and 30 mg L^{-1}), biosorbent dosage (2.5 mg L^{-1}, 5 mg L^{-1}, 10 mg L^{-1}, 15 mg L^{-1}, and 20 mg L^{-1}), temperature (15.0, 20.0, 25.0, 30.0 and 35 °C) and treatment time (from 0 to 240 min) initially screened under the same conditions as mentioned above. We adjusted pH by using 0.1 N HCl/NaOH, and in the experimental pH range, we focused on conditions below pH 5 to conform with typical acidic levels found in many industrial effluents, especially from tanneries, and to exploit the enhanced biosorption performance of microalgae in acidic environments due to increased electrostatic attraction forces between protonated biomass and anionic Cr(VI) species. This approach aligns the experimental framework with the most relevant scenarios for real-world industrial applications. All parameters were replicated five times. The elimination capacity of Cr(VI) from synthetic wastewater was measured after incubation.

Following each experiment, the samples were spun at 25,000× *g* for two minutes at a temperature of 4 °C to detach the solid biomass from the liquid medium. The biomass pellet was then extracted, and the remaining supernatant was preserved at −20 °C for subsequent examination. Cr(VI) levels in the supernatant were measured with the previously described method.

2.2.2. Optimization Adsorption Experiments

Drawing on batch experiment insights on Cr(VI) absorption, we homed in on three optimization variables: biosorbent dosage (A), treatment time (B), and pH level (C), and monitored their effect on reducing hexavalent chromium. We varied these variables at three distinct points (−1, 0, +1), as detailed in Table 1. A Response Surface Methodology (RSM) using a Box–Behnken Design, facilitated by Design Expert 13.0 software, was implemented to refine the Cr(VI) adsorption process. We explored how these independent variables collectively affected Cr(VI) removal efficiency. We applied a quadratic model to understand how each factor influenced the performance of Cr(VI) removal with the aid of microalgae. Parameters for biosorbent doses were set between 5 and 15 mg L^{-1}, with a treatment time of 90 to 150 min and a pH range from 0.5 to 2. We computed the Cr(VI) removal percentage using Equation (1).

Table 1. Experimental range and levels of the independent variables.

Independent Variables	Range and Levels		
	−1	**0**	**−2**
A (biosorbent dose, mg L^{-1})	5	10	15
B (Treatment time, min)	90	120	150
C (pH)	0.5	1	2

A mathematical model (Y), taking the form of a second-order polynomial quadratic equation (referred to as Equation (2)), was employed to analyze the principal and interactive effects of each variable.

$$Y = \beta_0 + \sum_{i=1}^{n} \beta_i X_i \sum_{i<1}^{n} \beta_{ij} X_i X_j + \sum_{j=1}^{n} \beta_{ij} X_j^2 \quad (2)$$

In this model, Y represents the Cr(VI) removal efficiency percentage; β_0 is intercepted, with β_i, β_{ij} and β_{jj} as the coefficients corresponding to linear, interaction, and quadratic terms, respectively. With three variables (n = 3) in the equation, Xi and Xj denote the independent variables, specifically pH, treatment time, and the biosorbent dose used.

The analysis revealed a precise fit of the model to the second-order response surface, with R^2 values confirming its predictive accuracy. The face-centered cubic design matrix,

alongside observed and predicted Cr(VI) removal rates, is detailed in Table 1. There was a close correlation between the uptake capacities measured experimentally and those forecasted by the quadratic model.

The optimization was validated under a 129.47 min treatment duration, with an optimal pH of 1.09 and a biosorbent dose of 10.91 mg L^{-1}.

2.2.3. Kinetic Study and Isotherm Studies

The experiments on the uptake kinetics were conducted in 250 mL Erlenmeyer flasks with 200 mL of synthetic wastewater within 10.0 mg L^{-1} Cr(VI) under optimal conditions. The cultivation parameters were identical to those described in Section 2.1 "Microalgae Absorption: Cultivation and Toxicity Test". All experiences were replicated five times. The three-milliliter sample was collected and examined at 30, 60, 90, 120, 150, 180, 210, and 240 min.

Adsorption curve experiments were carried out in 250 mL containers holding 200 mL of artificial wastewater under ideal conditions. The varying concentrations of Cr(VI) in the wastewater samples were set at 5, 10, 15, 20, 25, and 30 mg L^{-1}. All growth parameters were identical to those in Section 2.1. Therefore, five repetitions were given for all tests. After 24 h, wastewater samples (3 mL) were analyzed.

Two models described the kinetics and equilibrium of Cr(VI) sorption. Biosorption was described using pseudo-first- and pseudo-second-order models in nonequilibrium conditions. According to the differential Equation (3), the concept of liquid phase biosorption is encapsulated within the framework of the pseudo-first-order model [29].

$$-ln(q_e - q_t) = k_1 t - \ln(q_e) \quad (3)$$

where q is the amount of adsorbed solute, q_e is its value at equilibrium, k_1 (min^{-1}) is the pseudo-first-order rate constant, and t is the time.

Two surface sites are required in the pseudo-second-order Equation (4).

$$\frac{t}{q_t} = \frac{1}{K_2 q_e^2} + \frac{1}{q_e} t \quad (4)$$

in which k_2 ($g \cdot mg^{-1} \cdot min^{-1}$) is the pseudo-second-order constant kinetic rate.

Two isotherm models, the Langmuir (5) [30] (1918) and Freundlich (6) [31] equations, were compared to characterize the elimination of Cr(VI) by microalgae:

$$q_e = \frac{q_{max} \cdot K_L \cdot C_e}{(1 + K_L . C_0)} \quad (5)$$

$$q_e = K_F C_e^{\left(\frac{1}{nF}\right)} \quad (6)$$

Furthermore, the Langmuir isotherm was characterized using the Langmuir equilibrium constant (R_L), as delineated in Equation (7):

$$R_L = \frac{1}{1 + K_L C_0} \quad (7)$$

The value of R_L was determined by applying the numbers for K_L and C_0 in accordance with the stipulated relationship (referenced as Equation (7)). This R_L value is indicative of the adsorption process's characteristics, signaling whether it is favorable (when R_L is more than 0 but less than 1), linear (R_L equals 1), unfordable (R_L exceeds 1), or irreversible (when R_L equals 0) [32].

2.2.4. Characterization of the Biomass

The functional groups in the biomass determine the kinetics of biosorption because it is a process that favors physisorption. Therefore, the functional groups on the diatom cell

surface were examined using the Fourier Transmission Infrared (FTIR) spectrophotometer (Perkin Elmer FTIR-2000). Moreover, to analyze the algae subjected to Cr(VI) treatments from the experiments, FTIR (Fourier Transform Infrared Spectroscopy) assessments were conducted. For FTIR screening, pellets were prepared by blending 1 mg of the algal sample with 1 g of KBr in a 1:10 ratio. This mixture was then condensed into a solid form utilizing a bench press exerting 8 MT of pressure. The resulting FTIR spectra were recorded in the 500 to 4000 cm^{-1} [33]. Additionally, SEM-EDS (Scanning Electron Microscopy with Energy Dispersive X-ray Analysis) was employed to evaluate the changes in the microalgal biomass pre- and post-chromium treatment, utilizing an FEI Inspect F50 (FEI Instruments, Hillsboro, OR, USA) Inspect F50 scanning electron microscope equipped with an EDS detector for this analysis.

2.3. Desorption Studies

A series of five biosorption–desorption iterations were performed to evaluate the reusability of the biosorbent. For desorption, a solution of 0.1 M NaOH was used. The algal biomass, saturated with heavy metal ions, was subjected to the desorption process in the NaOH solution agitated on a rotary shaker at 120 rpm for two hours at a temperature of 25 °C. After each adsorption and desorption cycle, the algal mass was rinsed with milli-Q water and prepared for the next round of adsorption.

2.4. Data Analysis

The mean and standard errors of cell density and chromium (VI) levels in the solution were calculated using Microsoft Excel version 17.0. The relevance of the disparities in mean concentration levels was ascertained through variance analysis (ANOVA), with the significance level consistently maintained at 5%. Furthermore, to verify the presuppositions of ANOVA, such as the distribution's normalcy and the homogeneity of variances, IBM's SPSS software, version 20.0, was employed. Mean differences were evaluated using the *t*-test. Subsequently, the inhibitory concentration for 50% of microalgae cellular growth and the corresponding 95% confidence intervals were determined using nonlinear regression analysis in GraphPad Prism version 9.3.1. Lastly, graphs were produced with the help of Origin Pro 2020 by Origin Lab Corporation.

3. Results and Discussion

3.1. Absorption and Microalgae Tolerance to Cr(VI)

To investigate tolerance to hexavalent chromium, the microalgae *C. subminuscula* was cultivated in the absence and presence of Cr(VI) in concentrations between 0 and 30 mg L^{-1} (Figure 1). This microalga tolerated greater Cr(VI) concentrations; 48 h after introducing the Cr(VI), concentrations $\geq$ 10 mg L^{-1} had an impact on *C. subminuscula*'s growth. Despite the observed growth decrease for this Cr(VI), the microalgae survived for at least 10 days under Cr(VI) metal ion exposures. Cultures in the presence of 0 mg L^{-1}, 5 mg L^{-1}, or 10 mg L^{-1} Cr(VI) continued to grow logarithmically until around day 10, with no apparent change in cell density between these cultures (Student's *t*-test, $p = 0.271$). Moreover, the growth rates of *C. subminuscula* in the wastewaters with Cr(VI) concentrations of 5 and 10 mg L^{-1} were significantly the same as the control. Table 2 illustrates that the growth medium exposed to 5 and 10 mg L^{-1} Cr(VI) could undergo near-complete absorption, registering 99.94% and 96.48% for 5 and 10 mg L^{-1}, respectively. This suggests that the microalgae have the ability to thrive and proliferate in water with this chromium concentration. The growth medium does not exhibit toxicity towards the growth of the microalgae *C. subminuscula*. Algae possess the capability to detoxify metals through diverse mechanisms. This includes the first stage, when ion binding occurs at the cell surface. It is passive, fast, and reversible and occurs in living and nonliving cells. Proteins, carbohydrates and lipids of the microalgal cell wall are responsible for heavy metal adsorption via electrostatic interactions [34,35]. Simultaneously, alternative procedures in this phase incorporate the physical attraction of molecules, the swapping of ions, and the bond formation through chemisorption [34].

The second phase is characterized by the energy-requiring process of amassing metal ions internally within the cell. This phase is active, irreversible, somewhat protracted, and unique to living organisms. It is initiated when the external concentration of heavy metals notably surpasses the internal levels, prompting the movement of these metals into the cell membrane [35]. Yen et al. (2017) [36] observed a considerably elevated elimination of Cr(VI) by active microalgae when contrasted with mere metal adsorption observed in inactive cells. Metals can also be released inside the cells into the solution using an efflux system and the synthesis of phytochelatins or metallothioneins [37]. Tolerance is further facilitated by the deposition of metals in the cytoplasm and within vacuoles. Within the cytoplasm, metal concentrations are mitigated through the complexing or phytochelatin binding of metal ions, forming compounds of metallic sulfur, metallic iron, or metallic phosphate in the cytosol. Subsequently, these complexes are transported to vacuoles. Once inside the vacuoles, the acidic pH displaces the metal, allowing the peptide to re-enter the cytosol. Vacuoles, known for high concentrations of organic acids, trap the metal. This comprehensive strategy may function as a detoxification and cellular defense mechanism [38].

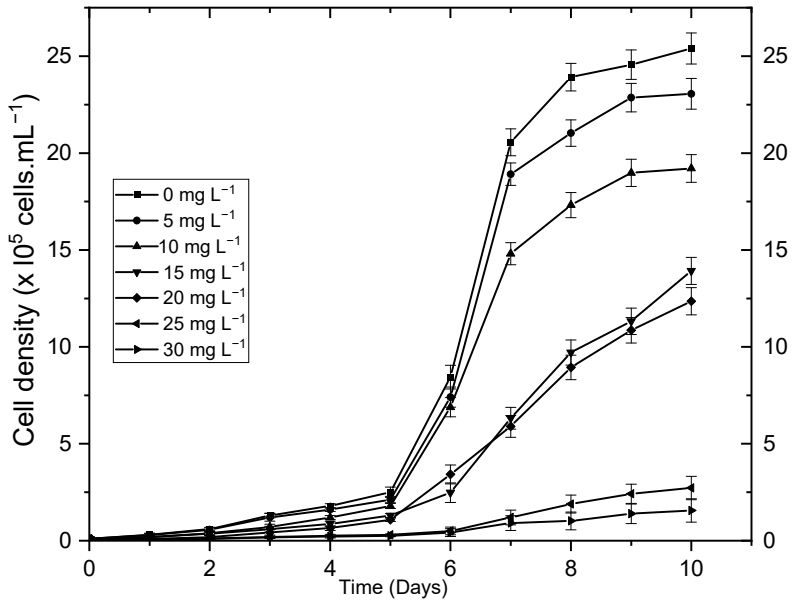

Figure 1. Growth curves of *Craticula subminuscula* in the absence or presence of Cr(VI). Mean ± SD of three biological replicates.

Table 2. Percentage of Cr(VI) ion removal with variations in concentration after toxicity test. Mean ± SD of three biological replicates.

	Concentration of Cr(VI) Ion Exposed (mg L^{-1})						
	0	**5**	**10**	**15**	**20**	**25**	**30**
Percentage of Cr(VI) biosorption	0	99.94 ± 0.71	96.48 ± 0.64	58.89 ± 0.87	23.44 ± 0.42	10.73 ± 0.31	8.21 ± 0.28

Metal transporters play a pivotal role as the primary defense mechanism for regulating osmotic balance. These transporters also regulate the internalization of ions vital for micronutrient homeostasis and mitigate the subsequent adverse effects of nonessential elements like Cr(VI) [39]. Various microalgae species have been reported to utilize several membrane transporters [40]. For instance, in *C. reinhardtii*, the movement of heavy metal ions (HMMs) from the extracellular environment to the cytosol can be facilitated by natural resistance-associated microphage proteins (NRAMP), the Fe-transporter (FTR), Zrt-Irt-like proteins (ZIP), and the copper transporter (CTR) [41]. These transporters have also been

identified in the vacuole membrane, which serves a similar role as assimilative transporters. Additionally, members of the cation diffusion facilitator (CDF), FerroPortiN (FPN), P1B-type ATPases, and the calcium (II)-sensitive cross-complementary 1/Vacuolar iron transporter 1 (Ccc1/VIT1) contribute to lowering the metal content in the cytoplasm by expelling active metal ions into the extracellular environment. Metal transporters play a crucial role in regulating metal concentrations within the cell, especially when the concentration exceeds cellular requirements or when metal–peptide complexes interfere with cellular metabolism [42].

In a recent study by Ferrari (2022) [43], the focus was placed on understanding sulfate transporters' role in the Cr(VI) resilience of Scenedesmus acutus. This research uncovered a clear link among the variable expression levels of these transporters, their behavior upon encountering Cr(VI), and the presence of sulfur, thereby endorsing the theory that the sulfate absorption and assimilation mechanisms are key in a cell's arsenal against metallic adversity. Notably, the SULTRs were found to be more active in sulfate-deprived variants. This mechanism seems to enhance chromium resistance by impeding the intake of Cr(VI) and promoting the generation of sulfur-bearing defensive molecules.

The study noted a steady trend of intensified ion uptake at Cr(VI) concentrations of 15 and 20 mg L^{-1}. Yet, cellular growth and the amount of Cr(VI) eliminated were less than observed when the exposure levels were at Cr(VI) concentrations of 5 and 10 mg L^{-1}. This suggests that while Cr(VI) ion absorption took place, it came with a side effect of toxicity (Figure 1 and Table 2). Chromium at these higher concentrations disrupted the growth of *C. subminuscula*. This disruption was attributed to the noncompetitive inhibition of the metal ion cofactor required by the enzymes, and the exchange of metal ions from the enzyme by complex reagents surpassed their tolerance limit [44,45]. At a Cr(VI) concentration of 25 mg L^{-1}, there was a sharp decline in the growth cells and absorption of Cr(VI), suggesting that the solution had become highly toxic to the microalgae, resulting in limited microbial growth. A similar trend was observed in the medium with a concentration of 30 mg L^{-1}, where minimal development of brown color occurred beyond the initial very pale brown shade (Figure 1 and Table 2). This serves as a biological marker indicating that the growth medium already possessed high levels of chromium ions [45].

In order to directly compare the effectiveness of this diatom with that of other different microalgae, we calculated the concentration of Cr(VI) required to reduce the cell density by 50% (IC50) using nonlinear regression. Compared to other species, the IC50 value for Cr(VI) calculated during the exposure period was 15.12 mg L^{-1}, which is much higher. For some authors, using diatoms for metal collection seems promising [46]. Our results indicate higher values for Cr(VI) when comparing these IC50 values to those shown for other microalgae such as *Navicula subminuscula*, *Scenedesmus incrassatulus*, *Planothidium lanceolatum*, *Chlorella vulgaris*, *Pseudokirchneriella subcapitata* and *Pseudokirchneriella subcapitata* [26,47–50]. Still, no toxicity study for *C. subminuscula* was conducted for such a comparison. Taken together, the toxicity data from the current and earlier studies show both similarities and differences. However, this cannot be avoided because comparing IC between different studies is typically tricky. Previous studies demonstrated that the Cr(VI) concentrations influencing microalgal growth are highly varied and dependent on other test conditions, such as cell densities and test media [51,52].

3.2. Adsorption Experiments

3.2.1. Single Factor Experiments

a. Effect of initial pH

Because the biosorbent's protonation determines the functional ion exchange sites and surface charge, the solution's starting pH is critical for hexavalent chromium uptake [41] (Sibi, 2016). The pH also regulates the adsorbate's charge. The microalgae contain hydrolyzable groups such as amines and aldehydes, as was discussed in the FTIR analysis. These two groups have more binding sites when acidified biomass and are easily protonated [42]. As a result, the pH of the solution was varied from 0.5 to 5.0 to study the influence of the

initial pH on Cr(VI) adsorption while other parameters were kept constant. Different initial pHs were used to evaluate the Cr(VI) uptake effectiveness and capacity during the pH change experiment. Figure 2 illustrates the uptake capacity and efficiency plot with starting solution pH. At pH 1.0, the highest uptake capacity was 277.48 mg g^{-1}. The pH increased consistently from 1.0 to 5.0, attaining 90.29 mg g^{-1} at pH 5.0.

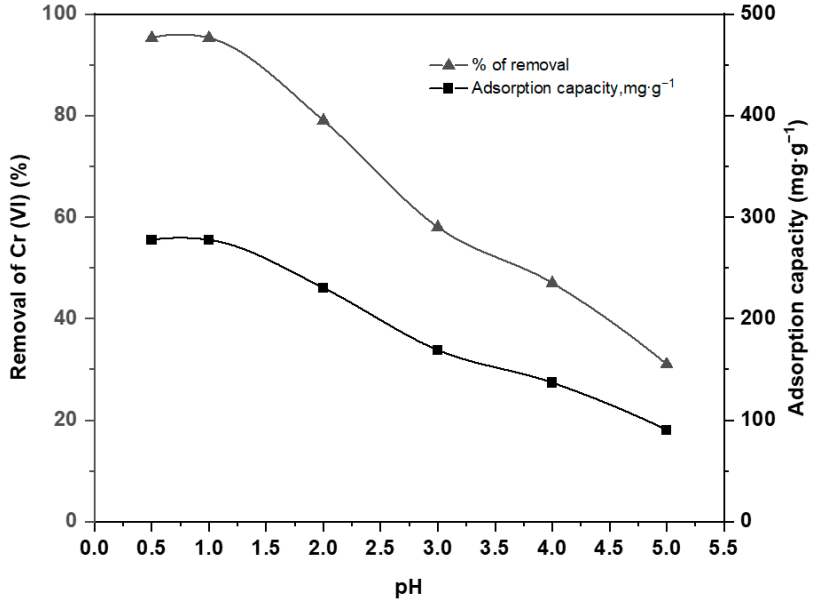

Figure 2. Effect of initial pH on the Cr(VI) biosoption. (Conditions: initial Cr(VI) conc., 10 mg L^{-1}; Algae biomass, 10 mg L^{-1}; contact time, 120 min; Temp., 25 °C; Light intensity, 67.5 μmol·m^{-2}·S^{-1}).

The highest Cr(VI) fixed on the protonated microalgae surface at acidic pH is favored by anionic adsorption [53]. At pH-1.0, the highest biosorption rate was 95.27%. At low pH values, amide, carboxyl, halide, and hydroxyl groups on biomass surfaces become protonated and positively charged [54]. Simultaneously, anionic Cr(VI) species, for example, dichromate ($Cr2O_7^{2-}$), chromate (CrO_4^{2-}), and tetraoxohydrochromate ($HCrO^{4-}$) ions formed under lower pH in the acidic solution [55]. The positively charged cell surface electrostatically adsorbed the anionic Cr(VI) species at lower pH ranges, causing significant physisorption of Cr(VI) on the microalgae [54]. As the proton concentration decreased as the pH of the solution increased, the fixation sites of the microalgae developed to be negatively charged. Due to electrostatic repulsion, negatively charged cells, compared with anionic chromate ions, cause lower uptake capacity at higher pH ranges [53]. The outcomes of the investigation into the influence of pH levels on the microalgae's ability to remove Cr(VI) from its environment indicate an optimal removal at notably acidic pH conditions.

This suggests that the algae eliminate this element through adsorption rather than absorption at this pH, which is unfavorable for the algae's survival. Consequently, as a continuation of this work, we conclude that the elimination of Cr(VI) of this microalgae is achieved through adsorption. Given this optimum, an implication arises for industrial wastewater treatment processes that typically exhibit a very low pH range around one, particularly in effluents from tanneries, as reported by Muthukkauppan and Parthiban [56], and around three, as mentioned by Lissaneddine et al. [57]. Although this is slightly more alkaline than the identified optimum of our study, it remains within a range conducive to high biosorption rates. This suggests that while industrial effluents may benefit from some degree of acidification, excessive pH modification may not be necessary. In addition, the environmental costs of such modifications, including potential ecological disruptions and compliance with discharge regulations, must be weighed against the incremental gains in decontamination efficiency. Hence, in the broader context of practical application, it becomes crucial to balance the theoretical maximal efficiency obtained under controlled

experimental conditions with the pragmatic, economic, and environmental realities of industrial operations.

b. Effect of contact time

Various contact times, ranging from 30 to 240 min, were conducted for the adsorption of Cr(VI) employing the *C. subminuscula* biomass while maintaining other constant parameters. The graph in Figure 3 illustrates the relationship between the contact time, the concentration of Cr(VI), and the percentage of its removal.

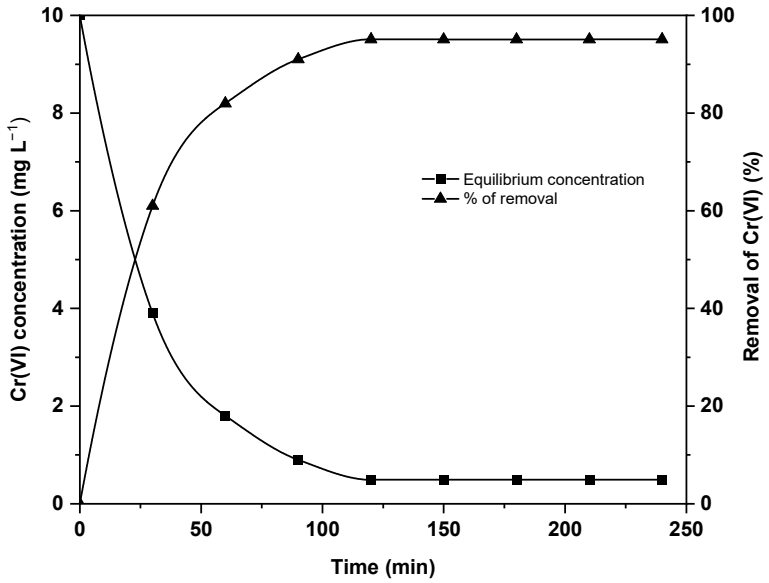

Figure 3. Effect of contact time on the Cr(VI) removal. (Conditions: initial Cr(VI) conc., 10 mg L^{-1}; Algae biomass, 10 mg L^{-1}; initial pH, 1.0; Temp., 25 °C; Light intensity, 67.5 μmol·m^{-2}·S^{-1}).

The bioremediation rate was extremely rapid, reaching a maximum of 90 min, with an adsorption percentage of just around 91%. Extending the exposure time to 240 min added just 4% additional Cr(VI). The rapid rate contributed to 91% of Cr(VI) uptake in just 90 min. After 90 min, the adsorption rate increased significantly, accounting for 95.1% removal up to 120 min. Hence, the equilibrium point of the adsorption experiment was thought to be at 120 min of biosorption. The biomass's finer particle size may cause a quick equilibrium time [58]. Therefore, the remaining adsorption tests modifying all parameters were performed for 120 min.

The first, quick phase could involve ions adhering physically or exchanging at the cell's surface, which precedes a more prolonged phase where other processes, such as compound formation, micro-precipitation, or the saturation of receptor sites, may occur. This two-stage process illustrates the diverse mechanisms at play when removing substances, showcasing the complexity of the interaction between the material and the cell [59]. Also notable is that various factors influence the adsorption rate, including the sorbate's and biosorbent's structural characteristics (e.g., composition of proteins and carbohydrates, surface charge density, topography, and surface area). Additionally, the quantity of biosorbent, the initial concentration of metal ions, and the presence of competing ions can impact the adsorption rate on active sites [59].

c. Effect of biosorbent dosage

The biosorbent quantity varied from 2.5, 5, 10, 15, and 20 mg L^{-1}. Figure 4 shows an adsorption capacity and efficiency graph plotted against algal biomass. With increased algae biomass from 2.5 to 10 mg L^{-1}, the removal efficiency of Cr(VI) increased rapidly from 49 to 95.29% and increased considerably to 20 mg L^{-1}, somewhat increasing to 96.3%. According to Bermudez et al. [60], the increased chromium found in smaller doses of

biomass is beneficial for industrial applications. Adding additional biosorbent increased the biosorption rate as algal biomass increased, creating a larger surface area.

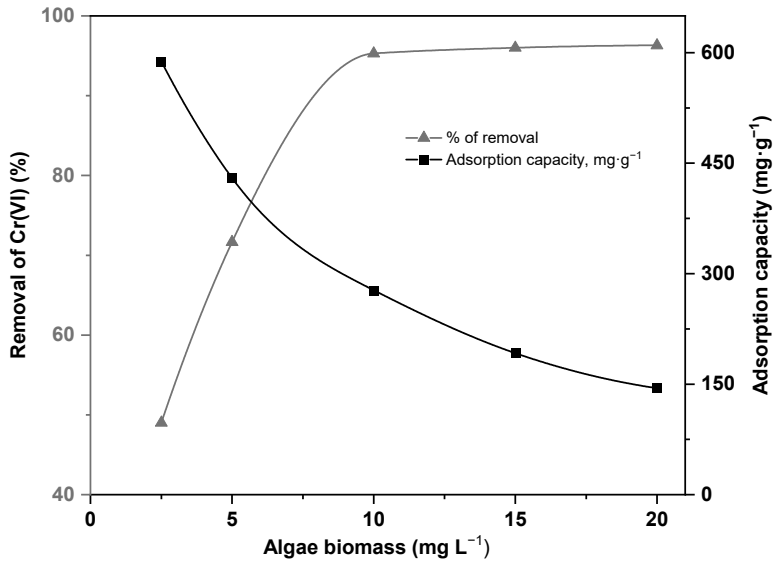

Figure 4. Effect of biosorbent dosage on the Cr(VI) removal. (Conditions: initial Cr(VI) conc., 10 mgL^{-1}; initial pH, 1.0; contact time, 120 min; Temp., 25 °C; Light intensity, 67.5 µmol·m^{-2}·S−^{1}).

In contrast, the flat increase in the biosorption rate observed with biosorbent doses of more than 10 mg L^{-1} was due to incomplete aggregation of the biomass particles because of a reduction in the effective surface area [59]. Maleki et al. [32] reported that a generally decreased biphasic interface causes biosorbent overlap or aggregation. Therefore, a biomass alga of 10 mg L^{-1} was selected as the optimal biosorbent quantity for Cr(VI) uptake. The adsorption capacity gradually reduced from 588 to 144.45 mg g^{-1} with increased algae biomass from 2.5 to 20 mg L^{-1}, respectively. The uptake rate decreased as the dosage of the algae biomass was increased (Figure 4), as determined by the quantity of hexavalent chromium uptake per gram of algae biomass (Equation (1)).

d. Effect of initial Cr(VI) concentration

The starting quantity of Cr(VI) as an adsorbate is significant in controlling the uptake rate because biosorption is a physical mass diffusion process that occurs at the interface of two phases [58]. The curve in Figure 5 shows an initial rapid adsorption that gradually slows down, suggesting adsorption is controlled by a diffusion process, such as physical mass diffusion. Although the initial increase in Cr(VI) concentration (5–10 mg L^{-1}) had no significant effect, the percentage uptake decreased from 98.3% to 95.3%. However, the starting Cr(VI) concentration rose from 10 to 30 mg L^{-1}, progressively reducing from 95.3% to 32.26%. Therefore, the optimal initial Cr(VI) concentration was 10 mg/L. When the initial Cr(VI) concentration was raised from 5 to 10 mg L^{-1}, the adsorption capacity doubled from 126.9 to 277.57 mg g^{-1}. When the concentration was elevated further up to 30 mg L^{-1}, practically nothing was modified. This could be due to a lack of binding sites in the microalgae to allow the growing quantity of Cr(VI) to diffuse, or their simultaneous contacts either restricted propagation of the two phases interface or their competitive attraction between them [61]. Bermdez et al. [59] suggest that the algal surface possesses a finite number of adsorptive sites. Upon saturation of these sites, further accumulation of Cr becomes unattainable.

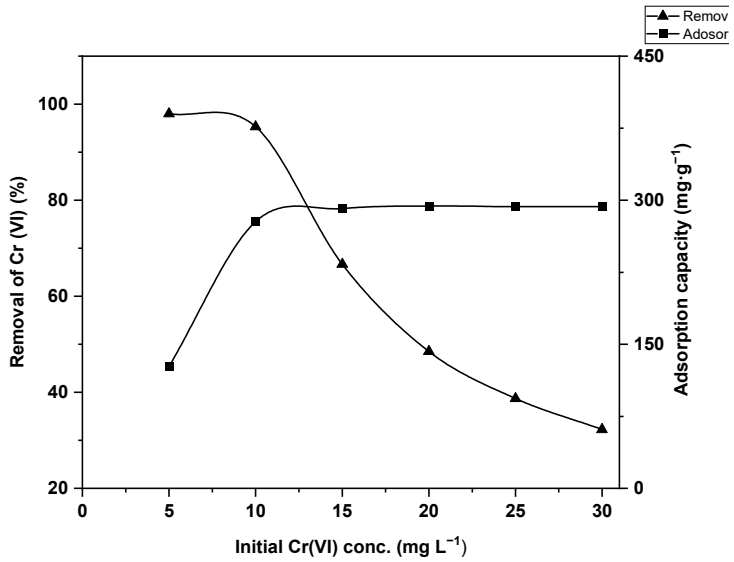

Figure 5. Effect of initial Cr(VI) concentration on the Cr(VI) removal. (Conditions: Algae biomass, 10 mg L^{-1}; initial pH, 1.0; contact time, 120 min; Temp., 25 °C; Light intensity, 67.5 µmol·m$-^{2}$·S^{-1}).

e. Effect of temperature

Physical adsorption starts thermodynamically at the interface of two phases based on the adsorption process [60]. It is determined by randomizing adsorbed molecules on the biosorbent's surface. Consequently, the temperature change is important in the randomness determination at the two-phase system interface. To assess the effect of the temperature variation for binding Cr(VI) to diatom biomass, the temperature was changed from 15 to 35 °C. Figure 6 depicts a graph that plots the relationship between temperature and adsorption efficacy and capacity, demonstrating an upward trend in biosorption performance as the temperature rises. As the temperature increased from 15 to 35 °C, the biosorption rate continuously increased from 75 to 96.9%. This might be because of the endothermic nature of the biosorption process [59]. The percentage of biosorption was enhanced with rising temperatures, potentially attributable to a surge in active groups on the biosorbent's surface or a reduction in the boundary layer's density around the microalgae, thereby making Cr(VI) more accessible to the active sites for binding, or possibly a combination of these factors [60].

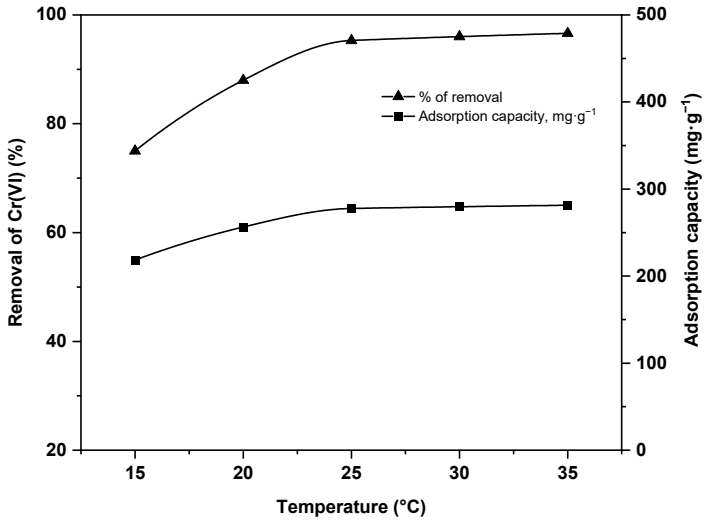

Figure 6. Effect of temperature on the Cr(VI) removal. (Conditions: initial Cr(VI) conc., 10 mg L^{-1}; Algae biomass, 10 mg L^{-1}; initial pH, 1.0; contact time, 120 min; Light intensity, 67.5 µmol·m^{-2}·S^{-1}).

3.2.2. Optimization of Cr(VI) Removal Conditions for *C. subminuscula*

Based on the batch experiments, three important conditions (biosorbent dosage, treatment time, and pH) were evaluated for more optimization. The RSM designed 15 treatments for the optimization experiments (Table 3). We notice that in treatment 8, the maximum Cr(VI) uptake efficiency was found with a Cr(VI) uptake efficiency of 95.32%. Using Design Expert 13.0 software, the experimental data were analyzed using multiple regression to create a quadratic multiple regression equation, shown in Equation (8).

$$Y = 94.70 + 1.75A + 1.04B - 4.66C + 0.57AB + 0.37AC - 0.16BC - 5.3A^2 - 4.34B^2 - 9.57C^2 \quad (8)$$

where Y is f Cr(VI) removal efficiency (%), A is the biosorbent dosage concentration (mg L^{-1}), B is the treatment time (min), and C is the pH.

Table 3. Box–Behnken design with the experimental responses.

Treatment	Factors and Their Levels			Observed Cr(VI) Removal (%)	Predicted Cr(VI) Removal (%)
	A	B	C		
	Biosorbent Dosage (mg L^{-1})	Treatment Time (min)	pH		
1	10 (0)	90 (−1)	0.5 (−1)	83.71	84.57
2	5 (−1)	150 (+1)	1 (0)	84.53	84.56
3	10 (0)	90 (−1)	2 (+1)	74.81	74.92
4	15 (+1)	150 (+1)	1 (0)	88.01	88.95
5	10 (0)	120 (0)	1 (0)	95.31	95.30
6	5 (−1)	90 (−1)	1 (0)	84.45	83.51
7	15 (+1)	120 (0)	2 (+1)	77.05	76.96
8	15 (+1)	120 (0)	0.5 (−1)	87.01	86.19
9	10 (0)	120 (0)	1 (0)	95.32	95.30
10	15 (+1)	90 (−1)	1 (0)	85.65	85.62
11	10 (0)	150 (+1)	2 (+1)	77.21	76.67
12	5 (−1)	120 (0)	0.5 (−1)	83.05	83.44
13	10 (0)	120 (0)	1 (0)	95.27	95.30
14	5 (−1)	120 (0)	2 (+1)	72.2	72.72
15	10 (0)	150 (+1)	0.5 (−1)	87.41	86.98

The analysis conducted to evaluate the validity of the quadratic multiple regression equation is detailed in Table 4. Based on the analysis, the equation proved extremely significant, as evidenced by an F-value of 99.13 and a *p*-value of less than 0.0001. It is essential for the model to present statistical significance (*p*-value less than 0.05) to fit the experimental design adequately. Conversely, a nonsignificant *p*-value (greater than 0.05) should correspond to the lack of fit factor [62].

In line with these criteria, the equation's "lack of fit" was deemed nonsignificant given its F-value of 1947.54 and *p*-value greater than 0.05, confirming a strong alignment between the regression equation and observed experimental results. A precision ratio of 30.577, significantly exceeding the threshold of 4, ensured a reliable signal, affirming the equation's capability to navigate the design space efficiently. The R^2 determination coefficient reaffirmed the significant relevance of the independent variables concerning the dependent variable, with a narrow gap observed between the predicted R^2 of 0.9112 and the adjusted R^2 of 0.9844, well under the 0.2 margin. In terms of individual factors, the regression analysis highlighted the importance of the biosorbent dosage (A), treatment time (B), and pH level (C) as significant contributors to the Cr(VI) removal efficiency, each with a *p*-value less than 0.05. However, the interactions amongst biosorbent dosage (A) and treatment time (B), dosage (A) and pH (C), as well as treatment time (B) and pH (C), did not demonstrate significance, as evidenced by *p*-values exceeding 0.05. On the other hand, the quadratic terms A^2, B^2, and C^2 each showed significant influence with *p*-values less than 0.01, as noted in Table 4.

Table 4. Analysis of variance of the quadratic multiple regression model for Cr(VI) removal efficiency.

Source	Sum of Squares	df	Mean Square	F-Value	*p*-Value	
Model	729.99	9	81.11	99.13	<0.0001	significant
A-biosorbent dosage	23.24	1	23.24	28.40	0.0031	
B-treatment time	8.22	1	8.22	10.05	0.0248	
C-pH	199.10	1	199.10	243.33	<0.0001	
AB	1.30	1	1.30	1.59	0.2632	
AC	0.5900	1	0.5900	0.7211	0.4346	
BC	0.1128	1	0.1128	0.1378	0.7257	
A^2	103.67	1	103.67	126.70	<0.0001	
B^2	69.59	1	69.59	85.04	0.0003	
C^2	254.40	1	254.40	310.91	<0.0001	
Residual	4.09	5	0.8182			
Lack of Fit	4.09	3	1.36	1947.54	0.11	nonsignificant
Pure Error	0.0014	2	0.0007			
Cor Total	734.08	14				

The effects and appropriate concentration of the three parameters for maximum Cr(VI) elimination efficiency were examined using a 3D response surface (Figure 7). The plots of the response surface illustrated the impact of each variable on the efficiency of chromium (VI) removal. By optimizing two factors and maintaining a third at its median z-axis value, we can observe their effects. In Figure 7i, you can see how the interplay between treatment duration (B) and pH level (C) unfolds when the biosorbent amount (A) is held constant at 10.91 mg L^{-1}. The combination of pH (C) and treatment duration had a significant effect on Cr(VI) biosorption capacity (B). Among increasing pH and time, the Cr(VI) uptake capacity primarily increased and then reduced due to excessively low or high pH levels that may reduce microalgae's ability to biosorbent metals [63].

When the treatment duration (B) was maintained at a mean of 128.47 min, the influence of the pH (C) and biosorbent quantity (A) on the efficiency of chromium (VI) removal was minor, as illustrated in Figure 7ii. An increase in pH and biosorbent levels either raised or lowered the efficiency of chromium (VI) removal, paralleling findings by Moreira et al. [63]. Figure 7iii further shows that holding the pH (C) at a median value of 1.09, the correlations between treatment time (B), biosorbent dosage (A), and chromium (VI) removal were marginal. Using Equation (8), optimal conditions for chromium absorption by *C. subminuscula* were determined. The peak removal efficiency for chromium (VI) was estimated at 95.30%, achieved at an ideal pH of 1.09, a biosorbent quantity of 10.91 mg/L, and a treatment span of 129.47 min. Verification of the optimization was conducted through a set of triplicate experiments at these optimal parameters. The findings showed negligible differences between the experimental and predicted values (p-value > 0.05), as reported in Table 5, affirming the model's reliability and possible replication.

Table 5. Validation of the optimum conditions for the microalga Cr(VI) removal.

Biosorbent Dosage (mg L^{-1})	Treatment Time (min)	pH	Predicted Value of Cr(VI) Removal (%)	Actual Value of Cr(VI) Removal (%)
10.913	129.47	1.09	95.30 [a]	95.32 [a]

[a]: No significant difference between the validated and predicted values (p-value > 0.05).

Biosorption experiments in batch culture were performed to maximize physicochemical factors (pH, temperature, agitation time, adsorbent dose, initial chromium concentration, and contact time). To optimize the chromium binding on the algae surface and to situate the performance of our tested species, Table 6 compares the uptake efficiency of Cr(VI) in the study with other studies in the literature. The Cr(VI) uptake efficiency by *C. subminuscula* was consistent with that by *Parachlorella kessleri* (96.1%) [64] and *Scenedesmus* sp.

(92.89%) [65], higher than that by *Planothidium lanceolatum* (about 87%) [26], *Chlamydomonas* sp. (91.31%) [66], *Scenedesmus quadricauda* (47.6%) [67], and *Chlorella vulgaris* (43%) [41], and lower than that by *Chlorella sorokiniana* (99.67%) [68], and *Scenedesmus quadricauda* (98.1%) [69]. It is clear from the table above that this alga has high metal binding capacities.

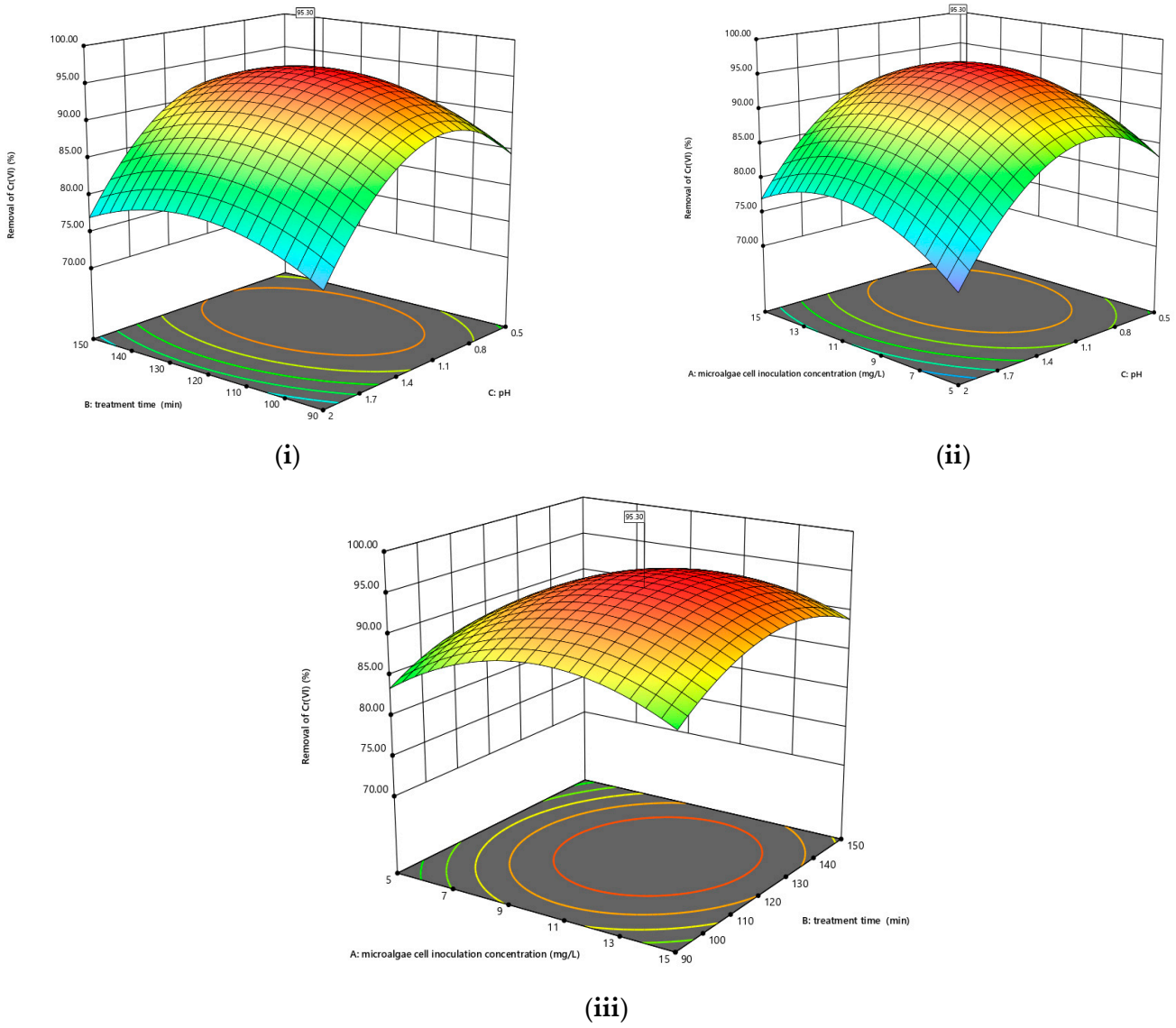

(**i**) (**ii**)

(**iii**)

Figure 7. Three-dimensional response surfaces and validation experiment. (**i**) Effects of pH (C) and time treatment (B), (**ii**) Effects of pH (C) and biosorbent dosage (A), (**iii**) Effects of time treatment (B) and biosorbent dosage (A). Spectrum color scale from blue to red means increasing removal percentage.

Table 6. Comparison of Cr(VI) removal efficiency by *C.subminuscula* with other microalgae species.

Microalgae Species	Heavy Metal	Conditions	Removal Efficiency (%)	Reference
Chlorella vulgaris	Cr(VI)	25 °C, pH = 2, biomass 1 g L^{-1}, [Cr(VI)] = 147 mg L^{-1}, time 240 min	43.00	[41]
Scenedesmus quadricauda	Cr(VI)	25 °C, pH = 1, biomass 2 g L^{-1}, [Cr(VI)] = 100 mg L^{-1}, time 120 min	47.6	[67]

Table 6. *Cont.*

Microalgae Species	Heavy Metal	Conditions	Removal Efficiency (%)	Reference
Planothidium lanceolatum	Cr(VI)	20 °C, pH = 1, biomass 0.4 g L^{-1}, [Cr(VI)] = 10 mg L^{-1}, time 30 min.	87.00	[26]
Chlamydomonas sp.	Cr(VI	[Cr(VI)] = 152 mg g^{-1}, time 30 min. pH = 4, biomass 1.5 g L^{-1}	91.31	[66]
Scenedesmus sp.	Cr(VI)	30 °C, pH = 1, [Cr(VI)] = 10 mg L^{-1}, time 120 min	92.89	[65]
Craticula subminuscula	Cr(VI)	25 °C, pH = 1.09, biomass 10.915 mg L^{-1}, [Cr(VI)] = 10 mg L^{-1},time 129.47 min.	95.30	This study
Parachlorella kessleri	Cr(VI)	Time196h Cr(VI)] = 30 mg L^{-1}, 23 °C	96.1	[64]
Scenedesmus quadricauda	Cr(VI)	Biomass 0.8 g L^{-1}, [Cr(VI)] = 5 mg L^{-1}, 25 °C, time 8 Days	98.1	[69]
Chlorella sorokiniana	Cr(VI)	[Cr(VI)] = 100 mg L^{-1}, time 1day. pH = 8, T° 40 °C, biomass 20 mL/100 mL	99.67	[68]

3.3. Kinetic and Isotherm Studies

The adsorption kinetics adequately reveal an effective operational period and other reaction mechanisms [70,71]. Therefore, the Cr(VI) uptake kinetics were evaluated under ideal parameters. Subsequently, the Cr(VI) absorption kinetics were analyzed optimally. To examine the kinetics of biosorption, both pseudo-first-order and pseudo-second-order models were applied (Table 7). A high coefficient of determination was noted for the pseudo-second-order model (R^2 = 0.9955), ruling out the possibility of pseudo-first-order kinetics being applicable (R^2 = 0.80). Regarding the pseudo-first-order and pseudo-second-order models, the calculated equilibrium biosorption capacities are 142.14 mg g^{-1} and 289.017 mg g^{-1}, respectively. The estimated equilibrium pseudo-second-order biosorption capacity was extremely similar to the experimental measurement, 277.57 mg g^{-1}. These findings showed that the pseudo-second-order model better explained the chromium (VI) biosorption kinetics in response to *C. subminuscula*. The findings align with outcomes reported in earlier studies [24,72,73].

Table 7. Adsorption isotherm coefficients for the Cr(VI) biosorption onto the microalgae biomass.

Kinetics Model	Coefficients	Value
	q_e experimental in mg g^{-1}	277.57
Pseudo first order	K_1 in min^{-1}	0.00011
	q_e calculated in mg g^{-1}	142.14
	R^2	0.80
Pseudo second order	k_2 in g·mg^{-1}·min^{-1}	0.0004
	q_e calculated in mg g^{-1}	289.017
	R^2	0.9955

Adsorption isotherms are thought to help understand how metal ions bind to adsorbent surfaces [74–80]. The equilibrium metal concentration in the biphasic system and metal biosorption per unit biomass at fixed temperature are correlated. It defines how metals interact and are distributed in the biphasic system at equilibrium [59]. It is determined by various factors, including the initial concentration of adsorbate, the quantity of biosorbent, the relative adsorption capacities, and the competition between solution compounds [42]. The Langmuir adsorption model, often applied in the study of biosorption, characterizes the formation of a single layer of various metals on biosorbent surfaces. It is commonly

employed to characterize diverse metal uptake on heterogeneous biosorbent materials. A modified version of this model is presented in Equation (4).

Using the experimental results, a linear plot $\frac{C_e}{q_e}$ of versus C_e was developed to determine the practicality of the Langmuir isotherm for Cr(VI) biosorption into algae cells (Figure 8a). The slope and intercept were used to estimate the values of q_{max} and K_L (Table 8). Equation (6) shows that the Langmuir isotherm was explained more by understanding the Langmuir equilibrium parameter (R_L). The R_L value was determined using equation (Equation (6)) values of K_L and C_0 and was obtained to be 0.0042. Based on the determined R_L value (0.0042), the biosorption of Cr(VI) with algae cells has proven favorable. Furthermore, an R_L value of less than one indicated that the uptake process was reversible [54].

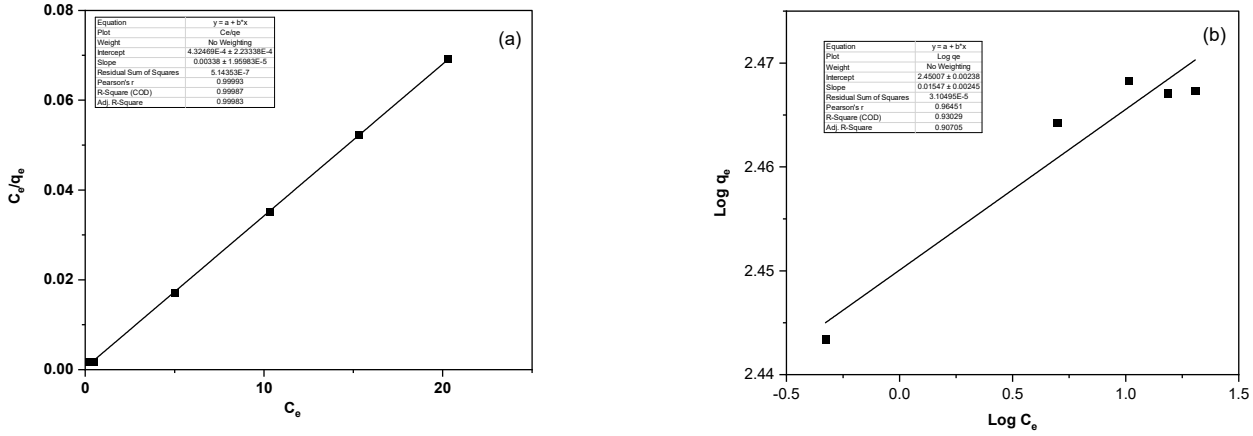

Figure 8. Adsorption isotherm curves: (**a**) Langmuir and (**b**) Freundlich.

Table 8. Data of the kinetic coefficients for Cr(VI) biosorption onto the microalgae biomass.

Langmuir Isotherm Model				Freundlich Isotherm Model		
q_{max} in mg g^{-1}	K_L in L·mg^{-1}	R_L	R^2	K_F in mg g^{-1}	$\frac{1}{n}$	R^2
295.85	7.81	0.0042	0.999	281.88	0.0155	0.907

The Freundlich adsorption isotherm explains the metal's arrangement in a solid–liquid biphasic system at the saturation level. A linear equation (Equation (5)) is used as a form to express the model in this sentence. To evaluate its utility for Cr(VI) biosorption, the experimental results were plotted as a linear plot of log(q_e) versus log(C_e) (Figure 8b). The values of $\frac{1}{n}$ and K_F (Table 7) were determined based on the plot's slope and intercept, respectively. The $\frac{1}{n}$ value characterizes the isotherm feasibility, e.g., irreversible ($\frac{1}{n} = 0$); favourable ($0 < \frac{1}{n} < 1$); and unfavourable ($\frac{1}{n} > 1$). The Freundlich isotherm model was favoured by the calculated $\frac{1}{n}$ value (0.0155). Both adsorption isotherm models were fitted using the correlation coefficients (R^2 values). They were found to be above 0.99 for the Langmuir isotherm model, indicating that the results of the isotherm analyses correspond reasonably to the Langmuir model [59]. Table 8 indicates that the Langmuir isotherm R_L value and the $\frac{1}{n}$ Freundlich adsorption isotherm value validated the ability of Cr(VI) biosorption on algal cells.

3.4. Thermodynamic Interpretation

The spontaneity of a biphasic biosorption process is defined by thermodynamic parameters such as Gibbs free energy (ΔG), enthalpy (ΔH), and entropy (ΔS) [59]. For example, the relation between ΔG, ΔH, ΔS, and absolute temperature (T) is illustrated in Equation (9) [60].

$$\Delta G = \Delta H - \Delta T \quad (9)$$

The law of thermodynamics may employ the ΔG values at various temperatures described in Equation (10) [32].

$$\Delta G = -RTln\,(K_C) \quad (10)$$

where K_c is the dimensionless equilibrium constant. Because the Langmuir constant (K_L = 7.81 L mg^{-1}) was determined in the preceding section, the K_c dimensionless value may be estimated using the equations presented in Equation (11) [81].

$$K_C = M_w.55.5.1000.K_L \quad (11)$$

Factor 55.5 is the number of moles of pure water per liter (1000 g/L divided by 18 g/mol). M_w is the molecular weight of the adsorbate (51,996 for Cr), and the term $M_w \times 55.5 \times 1000 \times K_L$ is dimensionless. The value of K_c was calculated using the formulae in Equation (11) and determined to be 22,554,098.4. The formulae in Equation (10) were used to calculate the ΔG values at various temperatures, and the results are shown in Table 8. The Van't Hoff equation was used to calculate the ΔH and ΔS [82]. However, in this article, they were calculated using Equation (9). A graph of ΔG plotted versus T gives a straight line, and the slope and intercept are, respectively, −ΔS and ΔH. The values of ΔH and ΔS were evaluated based on the fit of the experimental data to the plot, shown in Table 9.

Table 9. Thermodynamic parameters for the Cr(VI) biosorption onto microalgae biomass.

ΔG in kJ·mol^{-1}					**ΔH in kJ·mol^{-1}**	**ΔS in J·mol^{-1}·K^{-1}**	**R^2**
Temperature in K							
288	293	298	303	308			
−40.52	−41.22	−41.92	−42.63	−43.33	**-3.91×10^{-13}**	140.7	0.99

Within the experimental temperatures tested, the negative ΔG values indicate that the biosorption process occurs spontaneously [60]. The negative ΔG value indicated that the biomass had a higher concentration of Cr(VI) than the solution [54]. Also, its values demonstrated that spontaneity increased as temperature increased. According to Maleki et al. [32], the physisorption's G range should be between −20 and 0 kJ mol^{-1}, ranging from −80 to −400 kJ mol^{-1} in the chemisorption. The ΔG values at various temperatures, as shown in Table 9, indicated a combined physicochemical adsorption process in the biosorption mechanism [82]. The biosorption was unaffected by the substantially lower value of ΔH. However, the positive ΔS value indicated that the Cr(VI) uptake occurred due to the randomness of the adsorbate and biosorbent interface.

3.5. Characterization of the Biomass

The absorption of infrared radiation by functional groups on various organic macromolecules at unique wavelengths generates a detailed spectrum, often indicative of the cell's molecular composition [83,84]. Infrared spectra comparisons of algal cells, prior to and following exposure to 10 mg Cr(VI) per liter at a pH level of 1.0 for 120 min, are documented in Figure 9 and outlined in Table 10. Variations in peak intensities at distinct wave numbers, which differ based on the cultivation conditions of the *C. subminuscula* (Figure 9), have been detected. Notably, intense absorption bands reside near 1132 and 1074 cm^{-1}, predominantly associated with the vibrations of polysaccharide C-O bonds in algae treated with Cr(VI) (Table 10) [85,86]. Additionally, absorption bands at 1547 and 1654 cm^{-1} match the vibrational frequencies of N-H, C-N, and C=O bonds in amide groups found in proteins (Table 9). Stretching vibrations of the C=O bonds, characteristic of lipid esters and fatty acids, appear at 1745 cm^{-1}, with those emanating at 2854, 2928,

and 2950 cm^{-1} associated with the symmetric and asymmetric stretching of CH_2 and CH_3 groups in methyl and methylene chains of fatty acids (Table 10). As demonstrated by Wagner et al. [84], absorbance peak height, rather than the peak's integral, can quantify macromolecule concentrations. Consistent with what is documented through standard biochemical assays, an increase in lipid, carbohydrate, and protein content within algal cells is observed under Cr(VI) deficiency, compared to their standard growth conditions (Figure 9) [87].

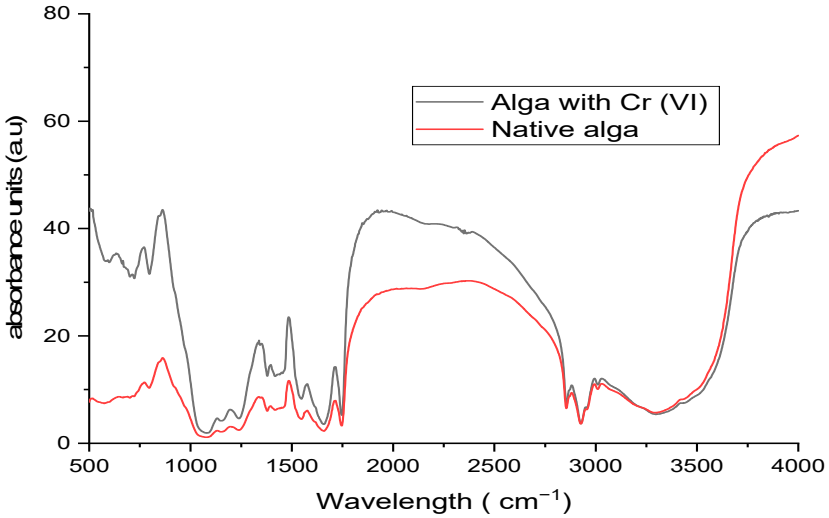

Figure 9. FTIR spectra of Cr(VI)-treated (black) and Cr(VI)-untreated (red) *C. subminuscula* based biosorbent.

Table 10. Band assignment and functional groups of a typical spectrum of *C. subminuscula* [59,65,88,89].

Wavenumber (cm^{-1})	Band Assignment & Functional Groups
3800–3000	$\sqrt{}$O-H of water, $\sqrt{}$N-H of amide, $\sqrt{}$C-O of carbohydrates
3028	$\sqrt{}$C-H of C=CH- chains of lipids
2950	$\sqrt{_{as}}CH_3$ of methyl groups
2928	$\sqrt{_{as}}CH_2$ of methylene
2854	$\sqrt{}CH_2$ and $\sqrt{}CH_3$ of methyl and methylene groups
1745	$\sqrt{}$C=O ester of lipids and fatty acids
1654	$\sqrt{}$C=O of proteins (Amide I)
1547	δN-H and $\sqrt{}$C-N of proteins (Amide II)
1450	$\delta_{as}CH_2$ and $\delta_{as}CH_3$ of methyl and methylene groups
1396	δCH_2 and δCH_3 from proteins and C-O from carboxylic groups
1232	$\sqrt{_{as}}$P=O from phosphodiester of nucleic acids and phospholipids
1200–1000	$\sqrt{}$C-O-C from polysaccharides
1075 & 950	Siloxane, silicate frustules
940	P-O-P of polyphosphates

Band assignment identity based on the work of Scarsini et al., [90] and Mayers et al., [86]; $\sqrt{}$ = symmetric stretching, $\sqrt{_{as}}$ = asymmetrical stretching, δ = symmetric deformation (bend), δ_{as} = asymmetric deformation (bend).

The investigation of *C. subminuscula* algae cells through scanning electron microscopy revealed their elliptical nature, measuring approximately 5–6 microns and exhibiting a rugged surface with well-defined micropores (Figure 10a). A comparison of cell morphology pre- and post-adsorption of Cr(VI) ions indicates a transformation from an irregular and porous structure, conducive to Cr(VI) ion adsorption, to a smoother surface (Figure 10b). Furthermore, noticeable alterations, such as shrinkage and layer adhesion induced by the impact of Cr(VI) ions, were observed after the adsorption of chromium ions on the cells.

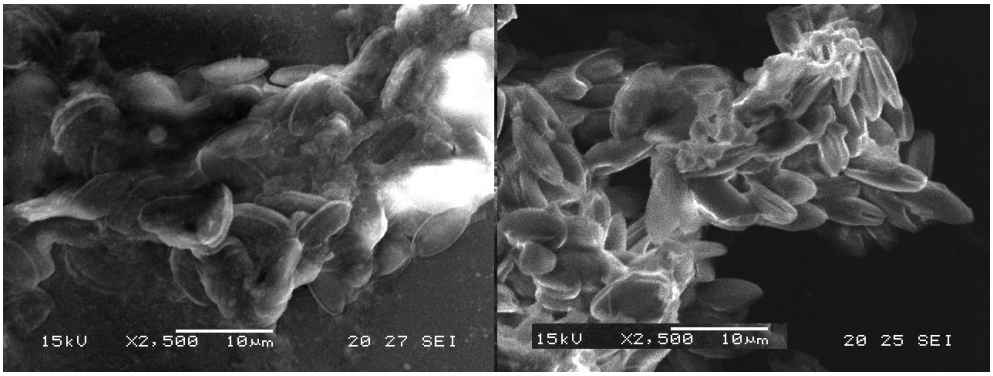

(**a**) (**b**)

Figure 10. SEM images of *C. subminuscula* cells surface (**a**) before and (**b**) after adsorption of Cr(VI) ions.

The use of the SEM–EDS technique showed that small amounts of chromium were concentrated on the surface of diatom cells after biosorption (Figure 11b), while this analysis was negative when the SEM–EDS technique was applied on the surface of *C. subminuscula* cells before biosorption (Figure 11a). Therefore, the EDS analysis indicates the biosorption of chromium by diatom *C. subminuscula* atomus.

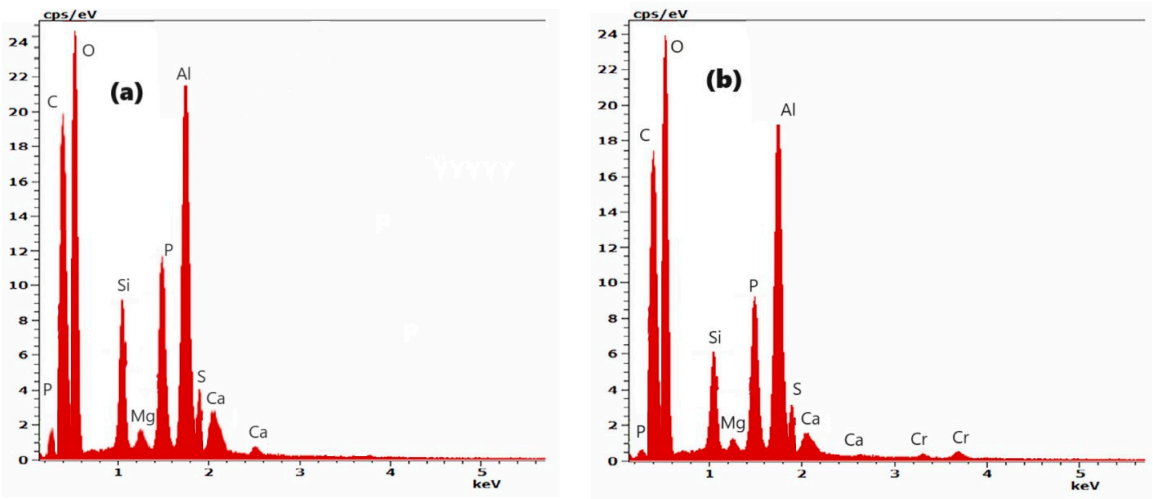

Figure 11. EDS analysis of the microalgae biomass: (**a**) before biosorption; (**b**) after biosorption.

3.6. Desorption Studies

The capacity to recycle biosorbents for continuous use is crucial for metal removal in wastewater treatment in industrial contexts. Trials utilizing *C. subminuscula* algal biomass treated with 0.1 M NaOH resulted in the successfully desorption of over 80% of the previously absorbed chromium from the algae. To evaluate the reusability of the biosorbent, a chromium adsorption–desorption cycle was conducted five times with the same batch. The binding efficiency of the various algal treatments exhibited considerable resilience, showing only a slight variation (maximum 10–15%) throughout the successive cycles of adsorption–desorption (Figure 12). This finding emphasizes the important aspect of biomass and adsorbent recyclability, highlighting its suitability for ongoing use in industrial applications.

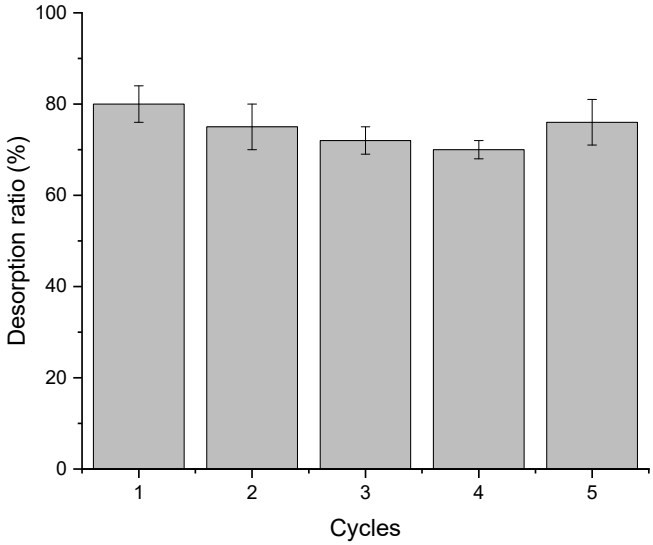

Figure 12. Desorption ratio of Cr from *C. subminuscula* at different desorption cycles using 0.1 M NaOH.

3.7. Post-Treatment of Biosorbent

A crucial step following microalgae's adsorption of hexavalent chromium is the post-treatment of the chromium-laden microalgae to prepare them for subsequent use in biofuel production. This section focuses on the methods employed for harvesting the biosorbent and the subsequent treatment processes to ensure safe handling and proper disposal of the contaminated biomass.

Firstly, we will address the harvesting of the adsorbed microalgae. Various methods can be used to harvest microalgae that have adsorbed hexavalent chromium from the treated water. The choice of technique depends on factors such as the type of microalgae, the intended application, and the production scale. For instance, benthic diatoms such as *C. subminuscula* are known for their ability to attach to solid surfaces, such as natural or artificial substrates. This property can be utilized to separate benthic diatoms from the decontaminated water. One example is adhesive supports specially designed to capture benthic diatoms when they come into contact with water containing these organisms. The diatoms adhere to these supports, allowing for their separation from the water. Once the diatoms are attached, the support can be removed, and the diatoms can be harvested [91,92].

Next, we will explore different methods for treating the harvested microalgae to reduce the concentration of adsorbed Cr(VI). Approaches such as washing the microalgae with complexing agents or buffer solutions can be employed to remove the adsorbed chromium and improve the quality of microalgae for their subsequent use.

Once the microalgae have been treated, they can be converted into biofuels through pyrolysis, hydroprocessing, or transesterification. These processes aim to transform the lipid components of microalgae into liquid biofuels, such as biodiesel, or gaseous biofuels, such as biogas [91,92].

We will highlight the potential benefits of this approach, including the opportunity to utilize the harvested microalgae within a circular economy where waste and by-products are valorized for renewable biofuel production. Furthermore, using microalgae as a biofuel feedstock offers environmental advantages, such as reduced greenhouse gas emissions and decreased reliance on fossil fuels.

In summary, the post-treatment of Cr(VI)-laden water using harvested microalgae provides a promising opportunity to harness these organisms for biofuel production. We will discuss the various steps involved in harvesting, treating, and converting microalgae, emphasizing the potential benefits of this approach in the realm of renewable energy.

4. Conclusions

The biomass of *C. subminuscula* microalgae exhibited notable proficiency in eliminating Cr(VI) from solutions when tested under ideal conditions (a pH level of 1.09, a biosorbent dose of 10.91 mg L^{-1}, and a treatment time of 129.47 min), achieving a chromium removal efficiency of 95.32%. The most accurate model to describe Cr(VI) biosorption in *C. subminuscula* was the pseudo-second-order model, which predicted a constant rate of 0.0004 and showcased theoretical and actual biosorption capacities of 289.01 mg g^{-1} and 277.57 mg g^{-1}, respectively. The spontaneous reaction proceeded thermodynamically due to the randomization at the biphasic interface of Cr(VI) ions. Langmuir and Freundlich isotherm models confirmed the feasibility of adsorption, and the Langmuir model provided a satisfactory fit for the biosorption process. The FTIR analysis confirms the existence of many functional groups in the biomass, including aldehydes, amides, carboxylic acids, phosphates, and halides, and SEM revealed that the surface cell has an irregular and porous structure conducive to Cr(VI) ion adsorption. Thus, the positive results of desorption cycles promise increased potential utilization of these algae in continuous systems within industrial processes. Additionally, it would be interesting to make a future attempt to use algal cells to produce high-performance and low-cost biosorbents for the uptake of Cr(VI) and other heavy metal ions from industrial wastewater effluents. The application of Cr(VI) biosorption on an in situ operating process and a pilot scale will also have to be given more consideration in the future.

Author Contributions: Conceptualization, K.S. and F.A.; methodology, S.E. and A.E.M.; software, K.A.; validation, K.S., F.A. and M.E.-S.; formal analysis, K.S.; investigation, F.A., S.L. and J.M.; resources, F.A.; data curation, K.S.; writing—original draft preparation, K.S.; writing—review and editing, F.A.; visualization, K.A.; supervision, K.S.; project administration, F.A. All authors have read and agreed to the published version of the manuscript.

Funding: This research was financed by the Morocco-Tunisian bilateral scientific cooperation project (20/PRD-02).

Institutional Review Board Statement: Not applicable.

Informed Consent Statement: Not applicable.

Data Availability Statement: Data is contained within the article.

Conflicts of Interest: The authors declare no conflict of interest.

References

1. Barrera-Díaz, C.E.; Lugo-Lugo, V.; Bilyeu, B. A review of chemical, electrochemical and biological methods for aqueous Cr(VI) reduction. *J. Hazard. Mater.* **2012**, *1–12*, 223–224. [CrossRef] [PubMed]
2. Bihuang, X.; Chao, S.; Zhe, X.; Xuchun, L.; Xiaolin, Z.; Jiajia, C.; Bingcai, P. One-step removal of Cr(VI) at alkaline pH by UV/sulfite process: Reduction to Cr(III) and in situ Cr(III) precipitation. *Chem. Eng. J.* **2017**, *308*, 791–797.
3. Ren, G.; Wang, X.; Huang, P.; Zhong, B.; Zhang, Z.; Yang, L.; Yang, X. Chromium (VI) adsorption from wastewater using porous magnetite nanoparticles prepared from titanium residue by a novel solid-phase reduction method. *Sci. Total Environ.* **2017**, *607–608*, 900–910. [CrossRef] [PubMed]
4. Belay, A.A. Impacts of Chromium from Tannery Effluent and Evaluation of Alternative Treatment Options. *J. Environ. Prot.* **2010**, *1*, 53–58. [CrossRef]
5. Huang, D.; Liu, C.; Zhang, C.; Deng, R.; Wang, R.; Xue, W.; Luo, H.; Zeng, G.; Zhang, Q.; Guo, X. Cr(VI) removal from aqueous solution using biochar modified with Mg/Al-layered double hydroxide intercalated with ethylenediaminetetraacetic acid. *Bioresour. Technol.* **2019**, *276*, 127–132. [CrossRef] [PubMed]
6. Bansal, M.; Singh, D.; Garg, V.K. A comparative study for the removal of hexavalent chromium from aqueous solution by agriculture wastes' carbons. *J. Hazard. Mater.* **2009**, *171*, 83–92. [CrossRef]
7. Cabatingan, L.K.; Agapay, R.C.; Rakels, J.L.L.; Ottens, M.; van der Wielen, L.A.M. Potential of Biosorption for the Recovery of Chromate in Industrial Wastewaters. *Ind. Eng. Chem. Res.* **2001**, *40*, 2302–2309. [CrossRef]
8. Dabrowski, A.; Hubicki, Z.; Podkościelny, P.; Robens, E. Selective removal of the heavy metal ions from waters and industrial wastewaters by ion-exchange method. *Chemosphere* **2004**, *56*, 91–106. [CrossRef]
9. Joo, S.H.; Tansel, B. Novel technologies for reverse osmosis concentrate treatment: A review. *J. Environ. Manag.* **2015**, *150*, 322–335. [CrossRef]

10. Peña-Castro, J.M.; Martínez-Jerónimo, F.; Esparza-García, F.; Cañizares-Villanueva, R.O. Heavy metals removal by the mi-croalga Scenedesmus incrassatulus in continuous cultures. *Bioresour. Technol.* **2004**, *94*, 219–222. [CrossRef]
11. Ahmad, S.; Pandey, A.; Pathak, V.V.; Tyagi, V.V.; Kothari, R. Phycoremediation: Algae as Eco-friendly Tools for the Removal of Heavy Metals from Wastewaters. In *Bioremediation of Industrial Waste for Environmental Safety: Volume II: Biological Agents and Methods for Industrial Waste Management*; Bharagava, R.N., Saxena, G., Eds.; Springer: Singapore, 2020; pp. 53–76. [CrossRef]
12. Muñoz, R.; Guieysse, B. Algal-bacterial processes for the treatment of hazardous contaminants: A review. *Water Res.* **2006**, *40*, 2799–2815. [CrossRef] [PubMed]
13. Yen, H.-W.; Chen, P.-W.; Hsu, C.-Y.; Lee, L. The use of autotrophic *Chlorella vulgaris* in chromium (VI) reduction under different reduction conditions. *J. Taiwan Inst. Chem. Eng.* **2017**, *74*, 1–6. [CrossRef]
14. Ajayan, K.V.; Selvaraju, M.; Unnikannan, P.; Sruthi, P. Phycoremediation of Tannery Wastewater Using Microalgae Scenedesmus Species. *Int. J. Phytoremediation* **2015**, *17*, 907–916. [CrossRef] [PubMed]
15. Napan, K. Influence of heavy metals from flue gas integration with algal production on biodiesel production. In *Graduate Research Symposium*; Utah State University: Logan, UT, USA, 2014; p. 80. Available online: https://digitalcommons.usu.edu/grs/80 (accessed on 6 October 2023).
16. Zhou, G.-J.; Ying, G.-G.; Liu, S.; Zhou, L.-J.; Chen, Z.-F.; Peng, F.-Q. Simultaneous removal of inorganic and organic com-pounds in wastewater by freshwater green microalgae. *Environ. Sci. Process. Impacts* **2014**, *16*, 2018–2027. [CrossRef] [PubMed]
17. Jácome-Pilco, C.R.; Cristiani-Urbina, E.; Flores-Cotera, L.B.; Velasco-García, R.; Ponce-Noyola, T.; Cañizares-Villanueva, R.O. Continuous Cr(VI) removal by Scenedesmus incrassatulus in an airlift photobioreactor. *Bioresour. Technol.* **2009**, *100*, 2388–2391. [CrossRef] [PubMed]
18. Travieso, L.; Cañizares, R.O.; Borja, R.; Benítez, F.; Domínguez, A.R.; Dupeyrón, R.; Valiente, V. Heavy metal removal by microalgae. *Bull. Environ. Contam. Toxicol.* **1999**, *62*, 144–151. [CrossRef] [PubMed]
19. Torres, E.M.; Hess, D.; McNeil, B.T.; Guy, T.; Quinn, J.C. Impact of inorganic contaminants on microalgae productivity and bioremediation potential. *Ecotoxicol. Environ. Saf.* **2017**, *139*, 367–376. [CrossRef]
20. Magro, C.D.; Deon, M.C.; Rossi, A.D.; Reinehr, C.O.; Hemkemeier, M.; Colla, L.M. Chromium (VI) biosorption and removal of chemical oxygen demand by Spirulina platensis from wastewater-supplemented culture medium. *J. Environ. Sci. Health Part A* **2012**, *47*, 1818–1824. [CrossRef]
21. Romera, E.; González, F.; Ballester, A.; Blázquez, M.L.; Muñoz, J.A. Comparative study of biosorption of heavy metals using different types of algae. *Bioresour. Technol.* **2007**, *98*, 3344–3353. [CrossRef]
22. Konwarh, R.; Pramanik, S.; Kalita, D.; Mahanta, C.L.; Karak, N. Ultrasonication—A complementary 'green chemistry' tool to biocatalysis: A laboratory-scale study of lycopene extraction. *Ultrason. Sonochem.* **2012**, *19*, 292–299. [CrossRef]
23. Konwarh, R.; Misra, M.; Mohanty, A.K.; Karak, N. Diameter-tuning of electrospun cellulose acetate fibers: A Box-Behnken design (BBD) study. *Carbohydr. Polym.* **2013**, *92*, 1100–1106. [CrossRef] [PubMed]
24. Sultana, N.; Hossain, S.M.Z.; Mohammed, M.E.; Irfan, M.F.; Haq, B.; Faruque, M.O.; Razzak, S.A.; Hossain, M.M. Experimental study and parameters optimization of microalgae based heavy metals removal process using a hybrid response surface methodology-crow search algorithm. *Sci. Rep.* **2020**, *10*, 15068. [CrossRef] [PubMed]
25. Guillard, R.R.L.; Lorenzen, C.J. Yellow-green algae with chlorophyllide $C^{1,2}$. *J. Phycol.* **1972**, *8*, 10–14. [CrossRef]
26. Sbihi, K.; Cherifi, O. Toxicity and biosorption of chromium from aqueous solutions by the diatom *Planothidium lanceolatum* (Brébisson) Lange-Bertalot. *AJSIR* **2012**, *3*, 27–38. [CrossRef]
27. Jobby, R.; Jha, P.; Yadav, A.K.; Desai, N. Biosorption and biotransformation of hexavalent chromium [Cr(VI)]: A comprehensive review. *Chemosphere* **2018**, *207*, 255–266. [CrossRef]
28. Eaton, A.D.; Clesceri, L.S.; Greenberg, A.E.; Franson, M.A.H. *Standard Methods for the Examination of Water and Wastewater*, 20th ed.; American Public Health Association: Washington, DC, USA, 1998.
29. Lagergreen, S. Zur Theorie der sogenannten Adsorption gelöster Stoffe. *Z. Für Chem. Ind. Kolloide* **1907**, *2*, 15. [CrossRef]
30. Langmuir, I. The adsorption of gases on plane surfaces of glass, mica and platinum. *J. Am. Chem. Soc.* **1918**, *40*, 1361–1403. [CrossRef]
31. Freundlich, H. Über die Adsorption in Lösungen. *Z. Für Phys. Chem.* **1907**, *57U*, 385–470. [CrossRef]
32. Maleki, A.; Naghizadeh, M.; Hayati, B.; Joo, S.W. Adsorption of hexavalent chromium by metal organic frameworks from aqueous solution. *J. Ind. Eng. Chem.* **2015**, *28*, 211–216. [CrossRef]
33. Langmuir, I. The constitution and fundamental properties of solids and liquids. Part I. *Solids. J. Am. Chem. Soc.* **1916**, *38*, 2221–2295. [CrossRef]
34. Monteiro, C.M.; Castro, P.M.; Malcata, F.X. Metal Uptake by Microalgae: Underlying Mechanisms and Practical Applications. *Biotechnol. Progr.* **2012**, *28*, 299–311. [CrossRef] [PubMed]
35. Suresh Kumar, K.; Dahms, H.-U.; Won, E.-J.; Lee, J.-S.; Shin, K.-H. Microalgae–A promising tool for heavy metal remediation. *Ecotoxicol. Environ. Saf.* **2015**, *113*, 329–352. [CrossRef]
36. Song, X.; Liu, B.F.; Kong, F.; Song, O.; Ren, N.Q.; Ren, H.Y. Simultaneous chromium removal and lipid accumulation by microalgae under acidic and low temperature conditions for promising biodiesel production. *Bioresour. Technol.* **2023**, *370*, 128515. [CrossRef] [PubMed]
37. Perales-Vela, H.V.; Peña-Castro, J.M.; Canizares-Villanueva, R.O. Heavy metal detoxification in eukaryotic microalgae. *Chemosphere* **2006**, *64*, 1–10. [CrossRef]

38. Shanab, S.; Essa, A.; Shalaby, E. Bioremoval capacity of three heavy metals by some microalgae species (Egyptian Isolates). *Plant Signal. Behav.* **2012**, *7*, 392–399. [CrossRef] [PubMed]
39. Juarez, A.B.; Barsanti, L.; Passarelli, V.; Evangelista, V.; Vesentini, N.; Conforti, V.; Gualtieri, P. In vivo microspectroscopy monitoring of chromium effects on the photosynthetic and photoreceptive apparatus of *Eudorina unicocca* and *Chlorella kessleri*. *J. Environ. Monit.* **2008**, *10*, 1313–1318. [CrossRef] [PubMed]
40. Basha, S.; Murthy, Z.; Jha, B. Biosorption of hexavalent chromium by chemically modified seaweed, Cystoseira indica. *Chem. Eng. J.* **2008**, *137*, 480–488. [CrossRef]
41. Sibi, G. Biosorption of chromium from electroplating and galvanizing industrial effluents under extreme conditions using Chlorella vulgaris. *GEE* **2016**, *1*, 172–177. [CrossRef]
42. Elangovan, R.; Philip, L.; Chandraraj, K. Biosorption of hexavalent and trivalent chromium by palm flower (Borassus aethiopum). *Chem. Eng. J.* **2008**, *141*, 99–111. [CrossRef]
43. Ferrari, M.; Cozza, R.; Marieschi, M.; Torelli, A. Role of Sulfate Transporters in Chromium Tolerance in *Scenedesmus acutus* M. (Sphaeropleales). *Plants* **2022**, *11*, 223. [CrossRef]
44. Daneshvar, E.; Zarrinmehr, M.J.; Kousha, M.; Hashtjin, A.M.; Saratale, G.D.; Maiti, A.; Vithanage, M.; Bhatnagar, A. Hexavalent Chromium Removal from Water by Microalgal-Based Materials: Adsorption, Desorption and Recovery Studies. *Bioresour. Technol.* **2019**, *293*, 122064. [CrossRef] [PubMed]
45. Susanto, A.; Kartika, R.; Koesnarpadi, S. Lead Biosorption (Pb) and Cadmium (Cd) by *Flavobacterium* Sp Bacteria. *Int. J. Sci. Technol. Res.* **2019**, *8*, 3611–3615.
46. Kunugi, M.; Sekiguchi, T.; Onizawa, H.; Jimbo, I. Utilization of Diatoms to Collect Metallic Ions. *Proc. Schl. Eng. Tokai Univ.* **2014**, *39*, 13–18.
47. Rai, P.K.; Tripathi, B.D. Removal of heavy metals by the nuisance cyanobacteria Microcystis in continuous cultures: An eco-sustainable technology. *Environ. Sci.* **2007**, *4*, 53–59. [CrossRef]
48. Deng, L.; Wang, H.; Deng, N. Photoreduction of chromium(VI) in the presence of algae, Chlorella vulgaris. *J. Hazard. Mater.* **2006**, *138*, 288–292. [CrossRef]
49. Rodgher, S.; Espíndola, E.L.G.; Simões, F.C.F.; Tonietto, A.E. Cadmium and Chromium Toxicity to Pseudokirch-neriella subcapitata and *Microcystis aeruginosa*, Braz. *Arch. Biol. Technol.* **2012**, *55*, 161–169. [CrossRef]
50. Cherifi, O.; Sbihi, K.; Bertrand, M.; Cherifi, K. The siliceous microalga *Navicula subminuscula* (Manguin) as a biomaterial for removing metals from tannery effluents: A laboratory study. *J. Mater. Environ. Sci.* **2017**, *8*, 884–893.
51. Wang, W.-X.; Dei, R.C.H. Influences of phosphate and silicate on Cr(VI) and Se(IV) accumulation in marine phytoplankton. *Aquat. Toxicol.* **2001**, *52*, 39–47. [CrossRef]
52. Rodríguez, M.C.; Barsanti, L.; Passarelli, V.; Evangelista, V.; Conforti, V.; Gualtieri, P. Effects of chromium on photosynthetic and photoreceptive apparatus of the alga *Chlamydomonas reinhardtii*. *Environ. Res.* **2007**, *105*, 234–239. [CrossRef]
53. Saha, B.; Orvig, C. Biosorbents for hexavalent chromium elimination from industrial and municipal effluents. *Coord. Chem. Rev.* **2010**, *254*, 2959–2972. [CrossRef]
54. Sathvika, T.; Manasi, V.; Rajesh, N. Rajesh, Adsorption of chromium supported with various column modelling studies through the synergistic influence of Aspergillus and cellulose. *J. Environ. Chem. Eng.* **2016**, *4*, 3193–3204. [CrossRef]
55. Pradhan, D.; Sukla, L.B.; Sawyer, M.; Rahman, P.K.S.M. Recent bioreduction of hexavalent chromium in wastewater treatment: A review. *J. Ind. Eng. Chem.* **2017**, *55*, 1–20. [CrossRef]
56. Muthukkauppan, M.; Parthiban, P. A study on the physicochemical characteristics of tannery effluent collected from Chennai. *Int. Res. J. Eng. Technol.* **2018**, *5*, 24–28.
57. Lissaneddine, A.; Aziz, K.; Ouazzani, N.; El Achaby, M.; Haydari, I.; Mandi, L.; Aziz, F. Continuous treatment of highly concentrated tannery wastewater using novel porous composite beads: Central composite design optimization study. *J. Environ. Health Sci. Engineer.* **2023**, *21*, 513–532. [CrossRef] [PubMed]
58. Gupta, V.K.; Rastogi, A. Biosorption of hexavalent chromium by raw and acid-treated green alga Oedogonium hatei from aqueous solutions. *J. Hazard. Mater.* **2009**, *163*, 396–402. [CrossRef] [PubMed]
59. González Bermúdez, Y.; Rodríguez Rico, I.L.; Guibal, E.; Calero de Hoces, M.; Martín-Lara, M.Á. Biosorption of hexavalent chromium from aqueous solution by Sargassum muticum brown alga. Application of statistical design for process optimization. *Chem. Eng. J.* **2012**, *183*, 68–76. [CrossRef]
60. Rezaei, H. Biosorption of chromium by using *Spirulina* sp. *Arab. J. Chem.* **2016**, *9*, 846–853. [CrossRef]
61. Meena, A.K.; Mishra, G.K.; Rai, P.K.; Rajagopal, C.; Nagar, P.N. Removal of heavy metal ions from aqueous solutions using carbon aerogel as an adsorbent. *J. Hazard. Mater.* **2005**, *122*, 161–170. [CrossRef]
62. Jaafari, J.; Barzanouni, H.; Mazloomi, S.; Amir, N.; Abadi Farahani, S.K.; Soleimani, P.; Haghighat, G.A. Effective adsorptive removal of reactive dyes by magnetic chitosan nanoparticles: Kinetic, isothermal studies and response surface methodology. *Int. J. Biol. Macromol.* **2020**, *164*, 344–355. [CrossRef]
63. Moreira, V.R.; Lebron, Y.A.R.; Freire, S.J.; Santos, L.V.S.; Palladino, F.; Jacob, R.S. Biosorption of copper ions from aqueous solution using Chlorella pyrenoidosa: Optimization, equilibrium and kinetics studies. *Microchem. J.* **2019**, *145*, 119–129. [CrossRef]
64. Bauenova, M.O.; Sadvakasova, A.K.; Mustapayeva, Z.O.; Kokociński, M.; Zayadan, B.K.; Wojciechowicz, M.K.; Balouch, H.; Akmukhanova, N.R.; Alwasel, S.; Allakhverdiev, S.I. Potential of microalgae Parachlorella kessleri Bh-2 as bio-remediation agent of heavy metals cadmium and chromium. *Algal Res.* **2021**, *59*, 102463. [CrossRef]

65. Pradhan, D.; Sukla, L.B.; Mishra, B.B.; Devi, N. Biosorption for removal of hexavalent chromium using microalgae *Scenedesmus* sp. *J. Clean. Prod.* **2019**, *209*, 617–629. [CrossRef]
66. Ayele, A.; Suresh, A.; Benor, S.; Konwarh, R. Optimization of chromium(VI) removal by indigenous microalga (*Chlamydomonas* sp.)-based biosorbent using response surface methodology. *Water Environ. Res.* **2021**, *93*, 1276–1288. [CrossRef] [PubMed]
67. Shokri Khoubestani, R.; Mirghaffari, N.; Farhadian, O. Removal of three and hexavalent chromium from aqueous solutions using a microalgae biomass-derived biosorbent. *Environ. Prog. Sustain. Energy* **2015**, *34*, 949–956. [CrossRef]
68. Husien, S.; Labena, A.; El-Belely, E.F.; Mahmoud, H.M.; Hamouda, A.S. Absorption of hexavalent chromium by green micro algae Chlorella sorokiniana: Live planktonic cells. *Water Pract. Technol.* **2019**, *14*, 515–529. [CrossRef]
69. Kafil, M.; Berninger, F.; Koutra, E.; Kornaros, M. Utilization of the microalga Scenedesmus quadricauda for hexavalent chromium bioremediation and biodiesel production. *Bioresour. Technol.* **2022**, *346*, 126665. [CrossRef]
70. Ahmed, W.; Mehmood, S.; Núñez-Delgado, A.; Ali, S.; Qaswar, M.; Khan, Z.H.; Ying, H.; Chen, D.-Y. Utilization of Citrullus lanatus L. seeds to synthesize a novel MnFe2O4-biochar adsorbent for the removal of U(VI) from wastewater: In-sights and comparison between modified and raw biochar. *Sci. Total Environ.* **2021**, *771*, 144955. [CrossRef]
71. Ahmed, W.; Mehmood, S.; Qaswar, M.; Ali, S.; Khan, Z.H.; Ying, H.; Chen, D.-Y.; Núñez-Delgado, A. Oxidized biochar obtained from rice straw as adsorbent to remove uranium (VI) from aqueous solutions. *J. Environ. Chem. Eng.* **2021**, *9*, 105104. [CrossRef]
72. Anastopoulos, I.; Kyzas, G.Z. Progress in batch biosorption of heavy metals onto algae. *J. Mol. Liq.* **2015**, *209*, 77–86. [CrossRef]
73. Liu, L.; Lin, X.L.; Luo, J.; Yang, J.; Luo, X.; Liao, H. Cheng, Biosorption of copper ions through microalgae from pig-gery digestate: Optimization, kinetic, isotherm and mechanism. *J. Clean. Prod.* **2021**, *319*, 128724. [CrossRef]
74. Ahmed, W.; Mehmood, S.; Núñez-Delgado, A.; Qaswar, M.; Ali, S.; Ying, H.; Liu, Z.; Mahmood, M.; Chen, D.-Y. Fabri-cation, characterization and U(VI) sorption properties of a novel biochar derived from Tribulus terrestris via two different approaches. *Sci. Total Environ.* **2021**, *780*, 146617. [CrossRef] [PubMed]
75. Ahmed, W.; Núñez-Delgado, A.; Mehmood, S.; Ali, S.; Qaswar, M.; Shakoor, A.; Chen, D.-Y. Highly efficient uranium (VI) capture from aqueous solution by means of a hydroxyapatite-biochar nanocomposite: Adsorption behavior and mechanism. *Environ. Res.* **2021**, *201*, 111518. [CrossRef]
76. Aziz, F.; Ouazzani, N.; Mandi, L.; Mamoun, M.; Uheida, A. Composite nanofibers of polyacrylonitrile/natural clay for decontamination of water containing Pb(II), Cu(II), Zn(II) and pesticides. *Sep. Sci. Technol.* **2017**, *52*, 58–70. [CrossRef]
77. Lissaneddine, A.; Pons, M.N.; Aziz, F.; Ouazzani, N.; Mandi, L.; Mousset, E. Electrosorption of phenolic compounds from olive mill wastewater: Mass transport consideration under a transient regime through an alginate-activated carbon fixed-bed electrode. *J. Hazard. Mater.* **2022**, *430*, 128480. [CrossRef] [PubMed]
78. Aziz, K.; El Achaby, M.; Mamouni, R.; Saffaj, N.; Aziz, F. A novel hydrogel beads based copper-doped Cerastoderma edule shells@Alginate biocomposite for highly fungicide sorption from aqueous medium. *Chemosphere* **2023**, *311*, 136932. [CrossRef]
79. Haydari, I.; Aziz, K.; Kaya, S.; Daştan, T.; Ouazzani, N.; Mandi, L.; Aziz, F. Green synthesis of reduced graphene oxide and their use on column adsorption of phenol from olive mill wastewater. *Process. Saf. Environ. Prot.* **2023**, *170*, 1079–1091. [CrossRef]
80. Elhamji, S.; Haydari, I.; Sbihi, K.; Aziz, K.; Elleuch, J.; Kurniawan, A.T.; Chen, Z.; Yap, P.S.; Aziz, F. Uncovering applicability of *Navicula permitis* algae in removing phenolic compounds: A promising solution for olive mill wastewater treatment. *J. Water Process. Eng.* **2023**, *56*, 104313. [CrossRef]
81. Tran, H.N.; You, S.-J.; Hosseini-Bandegharaei, A.; Chao, H.-P. Mistakes and inconsistencies regarding adsorption of contaminants from aqueous solutions: A critical review. *Water Res.* **2017**, *120*, 88–116. [CrossRef]
82. Liu, Y. Is the Free Energy Change of Adsorption Correctly Calculated? *J. Chem. Eng. Data.* **2009**, *54*, 1981–1985. [CrossRef]
83. Movasaghi, Z.; Rehman, S.; Rehman, I.U. Fourier Transform Infrared (FTIR) Spectroscopy of Biological Tissues. *Appl. Spectrosc. Rev.* **2008**, *43*, 134–179. [CrossRef]
84. Wagner, H.; Liu, Z.; Langner, U.; Stehfest, K.; Wilhelm, C. The use of FTIR spectroscopy to assess quantitative changes in the biochemical composition of microalgae. *J. Biophotonics.* **2010**, *3*, 557–566. [CrossRef] [PubMed]
85. Giordano, M.M.; Kansiz, P.; Heraud, J.; Beardall, B.; Wood, D. McNaughton, fourier transform infrared spectroscopy as a novel tool to investigate changes in intracellular macromolecular pools in the marine microalga chaetoceros muellerii (bacillariophyceae). *J. Phycol.* **2001**, *37*, 271–279. [CrossRef]
86. Mayers, J.J.; Flynn, K.J.; Shields, R.J. Rapid determination of bulk microalgal biochemical composition by Fourier-Transform Infrared spectroscopy. *Bioresour. Technol.* **2013**, *148*, 215–220. [CrossRef] [PubMed]
87. Huang, B.; Marchand, J.; Blanckaert, V.; Lukomska, E.; Ulmann, L.; Wielgosz-Collin, G.; Rabesaotra, V.; Moreau, B.; Bougaran, G.; Mimouni, V.; et al. Nitrogen and phosphorus limitations induce carbon partitioning and membrane lipid remodelling in the marine diatom *Phaeodactylum tricornutum*. *Eur. J. Phycol.* **2019**, *54*, 342–358. [CrossRef]
88. Hamad, H.; AbdElhafez, S.; Elsenety, M.; Sorour, M.K.; Amin, N.; Abdelwahab, O.; El-Ashtoukhy, E.-S. Fabrication and characterization of functionalized lignin-based adsorbent prepared from black liquor in the paper industry for superior removal of toxic dye. *Fuel* **2022**, *323*, 124288. [CrossRef]
89. Ali, R.; Elsagan, Z.; AbdElhafez, S. Lignin from Agro-Industrial Waste to an Efficient Magnetic Adsorbent for Hazardous Crystal Violet Removal. *Molecules* **2022**, *27*, 1831. [CrossRef]
90. Scarsini, M. The Transition Kinetic Toward Nitrogen Deprivation in the Marine Diatom Phaeodactylum tricornutum: A Multidisciplinary Approach. Ph.D. Thesis, Le Mans University, Le Mans, France, 2021. Available online: https://www.theses.fr/s206840 (accessed on 6 October 2023).

91. Milledge, J.J.; Heaven, S. A review of the harvesting of micro-algae for biofuel production. *Rev. Environ. Sci. Biotechnol.* **2012**, *12*, 165–178. [CrossRef]
92. Shamshad, K.; Naushad, M.; Jibra, I.; Chinna, B.; Gaurav, S. Production and harvesting of microalgae and an efficient operational approach to biofuel production for a sustainable environment. *Fuel* **2022**, *311*, 122543. [CrossRef]